Journal of Energy Storage 25 (2019) 100852

Contents lists available at ScienceDirect

Journal of Energy Storage

journal homepage: www.elsevier.com/locate/est

Advanced materials and technologies for hybrid supercapacitors for energy storage – A review

Ahmed Afif[a], Sheikh MH Rahman[b], Atia Tasfiah Azad[c], Juliana Zaini[a], Md Aminul Islan[d], Abul Kalam Azad[a,*]

[a] Universiti Brunei Darussalam, Faculty of Integrated Technologies, Jalan Tungku Link, Gadong, BE1410, Brunei Darussalam
[b] Chalmers University of Technology, Department of Chemistry and Chemical Engineering, Goteborg, SE, 41296, Sweden
[c] Department of Chemical Engineering, University of Aberdeen, AB24 3FX, UK
[d] Universiti Brunei Darussalam, Faculty of Science, Jalan Tungku Link, Gadong, BE1410, Brunei Darussalam

ARTICLE INFO

Keywords:
Supercapacitor
Energy storage
Graphene
Nanomaterials
Rechargeable battery

ABSTRACT

Supercapacitors have become the most significant energy conversion and storage system in recent renewable and sustainable nanotechnology. Due to its large energy capacity and supply with relatively short time and longer lifetime, supercapacitors breakthrough in advance energy applications. This review presents a comparative study of different materials, working principles, analysis, applications, advantages and disadvantages of various technologies available for supercapacitors. The aim of this article is to discuss the possibility of hybrid supercapacitor for the next generation of energy technology. The development of composite materials containing a wide range of active constituents (e.g., graphene, activated carbon, transition metals, metal oxides, perovskites and conducting polymers) by in-situ hybridization and ex-situ recombination is also discussed. This review consecrated largely the contribution of combining all materials (electrode and electrolyte) and their synthesis process and electrochemical performance. Enduringly, the potential issues and the perspectives for future research based on hybrid supercapacitors in energy applications are also presented.

1. Introduction

The expansion of renewable and sustainable energies has led to many small decentralized energy producers, such as wind power plants, hydropower plants and photovoltaic installations, being set up. It is now essential that flexible, lightweight, conductive materials with low-cost, CO_2 free and environmentally friendly energy conversion and storage systems are found in response to the needs of modern society and emerging ecological concerns [1–4]. Effective storage is necessary to be able to use these energy sources to cover the base load. Storage systems can be based on potential energy (e.g. pumped storage), pressure energy (e.g. compressed air storage), thermal energy (e.g. hot water reservoir), chemical or electrochemical energy (e.g. accumulator). Depending on the available energy, conversion into a storable form is also required, and reconversion if necessary. To increase the efficiency of a system, require kinetic energy to be stored somewhere whenever the system slows down or stops. These storage systems can be used in any energy devices, such as solar panels, batteries, fuel cells, Aluminum electrolytic capacitors, supercapacitors or in hydrogen storage. One of the great challenges in the twenty-first century is unquestionably energy storage. In response to the needs of modern society and emerging ecological concerns, it is now essential that new, low-cost and environmentally friendly energy conversion and storage systems are found; hence the rapid development of research in this field. The performance of these devices depends intimately on the properties of their materials. Innovative materials chemistry lies at the heart of the advances that have already been made in energy conversion and storage. To date, a lot of research has been done on energy storage materials and systems [5–8]. Unlike batteries, supercapacitors can be successfully performed with large amounts of power for efficiency enhancement as energy storage technologies [9]. Due to their high-power capabilities and long cycle-life, these have attracted significant attention, giving a very good chance to build more advanced hybrid supercapacitors, for both on-board and stationary applications such as electrochromic, hybrid battery, thermally chargeable, self-healing, shape memory, piezoelectric etc [10]. Electrolytic capacitors feature unlimited charge/discharge cycles, high dielectric strength and good frequency response as AC resistance in the lower frequency range. Supercapacitors can store 10–100 times more energy than electrolytic capacitors, but they do not support AC applications. With regards to

* Corresponding author.
E-mail address: abul.azad@ubd.edu.bn (A.K. Azad).

https://doi.org/10.1016/j.est.2019.100852
Received 5 April 2019; Received in revised form 8 July 2019; Accepted 25 July 2019
Available online 31 July 2019

rechargeable batteries supercapacitors feature higher peak currents, low cost per cycle, no danger of overcharging, good reversibility, non-corrosive electrolyte and low material toxicity, while batteries offer, lower purchase cost, stable voltage under discharge, but they require complex electronic control and switching equipment, with consequent energy loss and spark hazard given a short.

Though much of the most ground-breaking research has been done relatively recently, the original concept of SCs dates to the 19th century. Today, the performance of SCs has been drastically improved, but there are still aspects that can be significantly enhanced. The actual performance of a supercapacitor device is frequently being measured by the power density and energy density of the system. Much of the research being done and still going on SCs concerns the improvement of these performance metrics along with other key performance metrics, such as charge-discharge cycle, series/charge transfer resistance, frequency response, materials miniaturization etc [11–13]. The efficiency and performances of SCs in applications can be improved by improving the voltage window, the superior cycling stability and miniaturization of supercapacitors and their integration on chips or flexible, lighter and transparent substrates [14,15]. There have been many studies on the employment of electrode material for supercapacitor. The activated carbons, conducting polymers and transition metal oxides are still the generally used as electrode materials [10]. This review focuses on the different types of SCs, providing a summary of advances and comparisons. Furthermore, we briefly discuss the uses and technical challenges for developing electrode materials (carbon-based materials, metal oxides, perovskites, conducting polymers and hybrid), electrolyte choices and perspectives for future research.

2. Supercapacitors

The scientific community is focusing on energy due to the changing global landscape. In this regard more, efforts are related to the developing and refining of the energy storage devices. Recently, supercapacitor (SC) has been attracted as an energy storage device like a battery in design and manufacture. The SCs are also called ultracapacitors or electrochemical capacitors, utilize high surface area electrode materials and thin dielectrics to achieve higher capacitance as compared to the conventional capacitors [16–19]. Batteries and capacitors seem similar as they both store and release electrical energy. However, the crucial differences between them are how they function differently on set-up applications. Different battery types are distinguished by their chemical makeup. The chemical unit, called the cell, contains three main parts; a positive terminal called the cathode, negative terminal called the anode, and the electrolyte. The battery charges and discharges through a chemical reaction that generates a voltage. The battery can provide a consistent DC voltage. In rechargeable batteries, the chemical energy that is converted into electricity can be reversed using outside electrical energy to restore the charge. However, in general, batteries provide higher energy density for storage, while capacitors have more rapid charge and discharge capabilities [20]. Supercapacitor, an upgrade version of the capacitor, can be successfully performed with large amounts of power for efficiency enhancement as energy storage technologies [9]. Due to their high-power capabilities and long cycle-life (> 100 times battery life), these have attracted significant attention, giving a very good chance to build more advanced hybrid ESSs, for both on-board and stationary applications. Table 1 compares the major parameters of the three main supercapacitor families with electrolytic capacitors and batteries [21].

In the future, the SC can be used either in conjunction with batteries or replace batteries in the storage system (continuous power supply, and load leveling). Recently electrochemical double layer capacitors (EDLCs) were used in emergency doors on an airbus A-380 with providing the safety, performance and reliability issues [22,23]. For the future energy storage systems, both SC and batteries are given equivalent importance by US Department of Energy. The general public shows great interest in the articles published on SC in popular magazines [24,25].

In a conventional Lithium-ion battery, the electrochemical reaction happens differently during discharging and charging period. In the discharging period, battery works as a load. Working Lithium electrons flow through separator from the anode (negative electrode) to cathode (positive electrode). In charging period, battery works charger in where electrons flow cathode to the anode. Similarly, in conventional capacitors, insulating dielectric material separated the two conducting electrodes. Opposite charges accumulate on the surface of each electrode as the voltage is applied to the capacitor. The dielectric keeps the charges separated, by creating an electric field that allows the capacitors to store energy. This is depicted in Fig. 1 (a). Fig. 2 shows the regone plot of performance ranges of various energy storage devices.

Capacitance C is defined as the ratio of stored (positive) charge Q to the applied voltage V:

$$C = Q / V \tag{1}$$

For a conventional capacitor, C is directly proportional to the surface area A of each electrode and inversely proportional to the distance D between the electrodes:

$$C = \varepsilon_0\ \varepsilon_r\ A / D \text{ or } C/A = \varepsilon_0\ \varepsilon_{r\ /\ D} \tag{2}$$

Where ε_0 = dielectric constant of free space and ε_r = dielectric constant of insulating material between electrodes. The energy E stored in a capacitor is directly proportional to its capacitance

$$E = \tfrac{1}{2}\ CV^2 \tag{3}$$

In general, the Power is the energy expended per unit time. For capacitor power determination, the SC is mainly considered as a series circuit with external load resistance R as shown in Fig. 3 (b). The internal components of the capacitors (e.g. current collector, electrodes, and dielectric material) also contribute to the resistance which is measured in aggregate by a quantity known as the equivalent series resistance (ESR). The voltage during discharge is determined by these resistances. When measured at matched impedance (R = ESR) the maximum power P max for a capacitor is given by

$$P = V^2 / 4 \times ESR \tag{4}$$

This relation shows how the ESR can limit the maximum power of a capacitor [16,19,26]. Capacitors store less energy per unit mass or volume, but they deliver a lot of power, as the power density is usually high. SC is governed by the same basic principles as the conventional ones. But as the higher surface area of electrodes and no dielectric between plates; rather, an electrolyte and a thin insulator are used the capacitance and energy increase by using the above equations. The performance improvement for SC is shown in Fig. 2 a graph termed as Ragone plot, where power density is measured along the vertical axis versus energy density on the horizontal axis [27]. This power vs energy density graph is an illustration of the comparison of various power devices storage, where it is shown that SC occupy the region between conventional capacitors and batteries.

Specific capacitance (C_s) is used to reflect the property of the active material on a single electrode. It is most reliably measured by the three-electrode cell but can also be derived from the two-electrode cell.

For a commercial symmetrical supercapacitor,

$$C_s = \frac{4 \times C_{cell}}{a\ \% \times W_{cell}} \tag{5}$$

where, C_{cell} is the cell capacitance, W_{cell} is the overall weight of the device, and a% is the percentage of active material mass over the overall cell weight. For the commercial asymmetrical cell, to calculate the specific capacitance of each electrode material, the masses of the active materials on both the positive electrode and negative electrode must be known with C_{cell} and W_{cell}.

Table 1
Parameters of supercapacitors compared with electrolytic capacitors and lithium-ion batteries.

Parameter	*Aluminum electrolytic capacitors*	*Supercapacitors*			*Lithium-ion batteries*
		Double-layer capacitors for memory backup	Super-capacitors for power applications	Pseudo and Hybrid capacitors (Li-Ion capacitors)	
Temperature range (°C)	−40 to +125	−40 to +70	−20 to +70	−20 to +70	−20 to +60
Cell voltage (V)	4 to 630	1.2 to 3.3	2.2 to 3.3	2.2 to 3.8	2.5 to 4.2
Charge/discharge cycles	unlimited	10^5 to 10^6	10^5 to 10^6	$2 \cdot 10^4$ to 10^5	500 to 10^4
Capacitance range (F)	≤ 2.7	0.1 to 470	100 to 12000	300 to 3300	—
Specific energy (Wh/kg)	0.01 to 0.3	1.5 to 3.9	4 to 9	10 to 15	100 to 265
Specific power (kW/kg)	> 100	2 to 10	3 to 10	3 to 14	0.3 to 1.5
Self-discharge time at room temperature	short (days)	middle (weeks)	middle (weeks)	long (month)	long (month)
Efficiency (%)	99	95	95	90	90
Life time at room temperature (years)	> 20	5 to 10	5 to 10	5 to 10	3 to 5

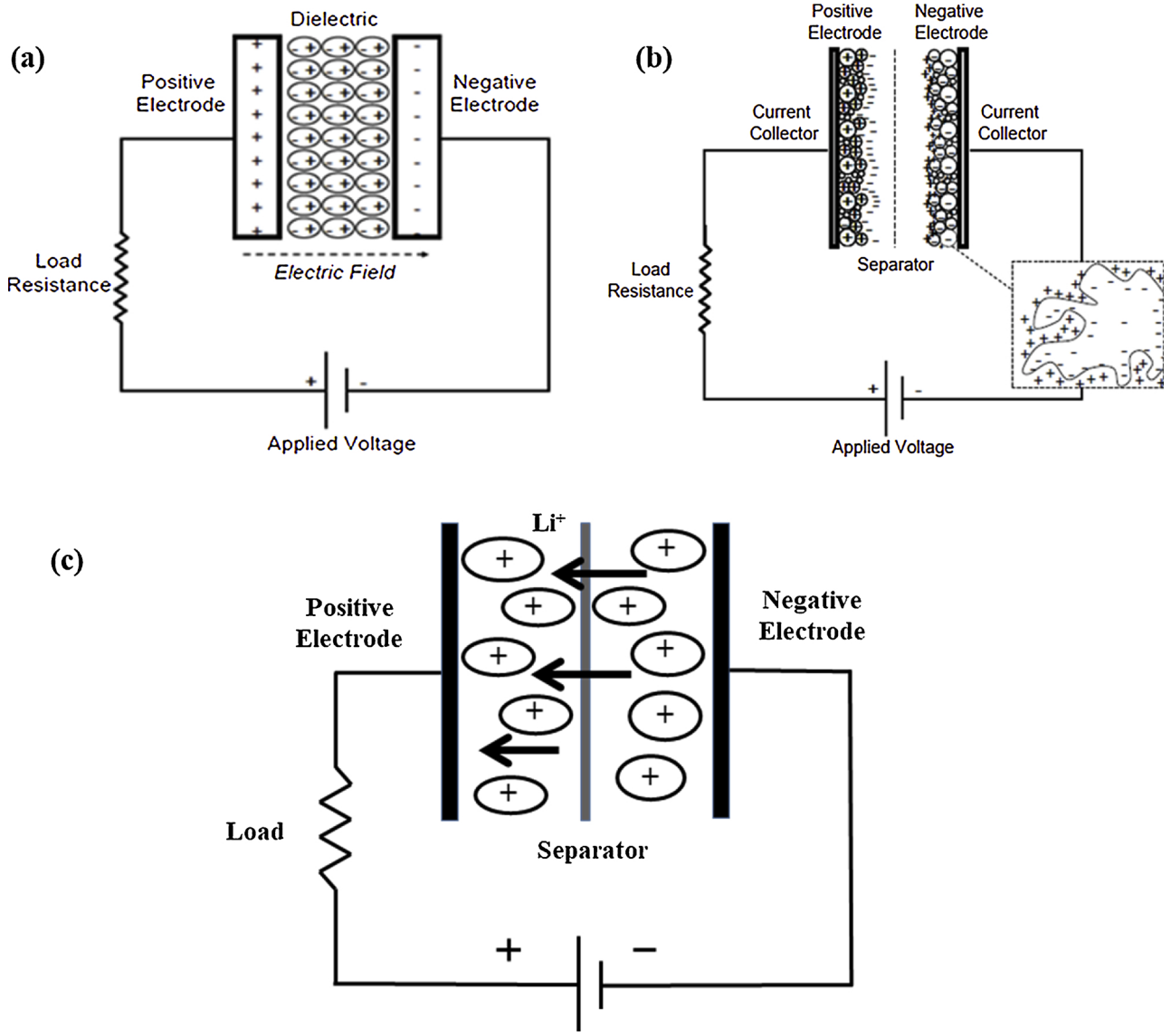

Fig. 1. (a) Schematic of conventional capacitor, (b) Schematic of an electrochemical double layer capacitor and (c) Schematic of conventional discharging battery.

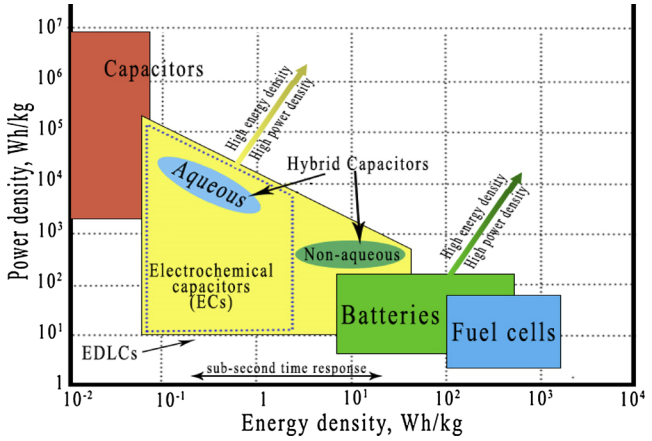

Fig. 2. Ragone plot of performance ranges of various energy storage devices.

As for the difference in material loading on the electrode, the value is usually high (> 1 mg/cm^2) in commercial supercapacitors, whilst the reported data in literature was measured from electrode with mass loading being < 0.1 mg/cm^2 which can produce over estimated specific capacitance due to contribution from the surface of the current collector [28].

Though the SCs exhibit greater capacitance than conventional capacitors yet SC must meet the demands of batteries and fuel cell regarding energy density. Supercapacitors are used in applications requiring many rapid charge/discharges cycles rather than long term compact energy storage: within cars, buses, trains, cranes and elevators, where they are used for regenerative braking, short-term energy storage or burst-mode power delivery. Smaller units are used as memory backup for static random-access memory (SRAM). Supercapacitors do not use the conventional solid dielectric of ordinary capacitors. They use electrostatic double-layer capacitance and electrochemical pseudocapacitance, both of which contribute to the total capacitance of the capacitor, however, with different amounts. The structure-property relationship is very important to introduce and discuss the materials of SCs. The porosity and surface area are the main booster for electrical double layer capacitance, while redox charge transfer contributes significantly to pseudo capacitance [29,30]. Supercapacitors can be classified into the following classes based on charge storage phenomenon. Fig. 3 exhibits different types of supercapacitors. Supercapacitors can be made in different geometrical forms, such as thin film and sandwich type as flexible supercapacitors and integrated micro-supercapacitors as planar supercapacitors. Flexible supercapacitors are super-fast rechargeable electrochemical energy storage device, combining the advantages of high storage capability and power output as well as high malleability without any significant performance loss. Thus, flexible supercapacitors require electrode materials not only with good electrochemical properties, but also with high mechanical integrity upon bending or folding, compact design and lightweight property. The planar configuration design offers planar channels for electrolyte ions, facilitating fast ion transport in the two-dimensional direction. This type of supercapacitors pushes the performance of flexible supercapacitors to a higher level [31–33]. Depending on the electrode materials supercapacitors can be divided in 3 categories (see Fig. 3) (i) Electrochemical double layer supercapacitors, (ii) Hybrid

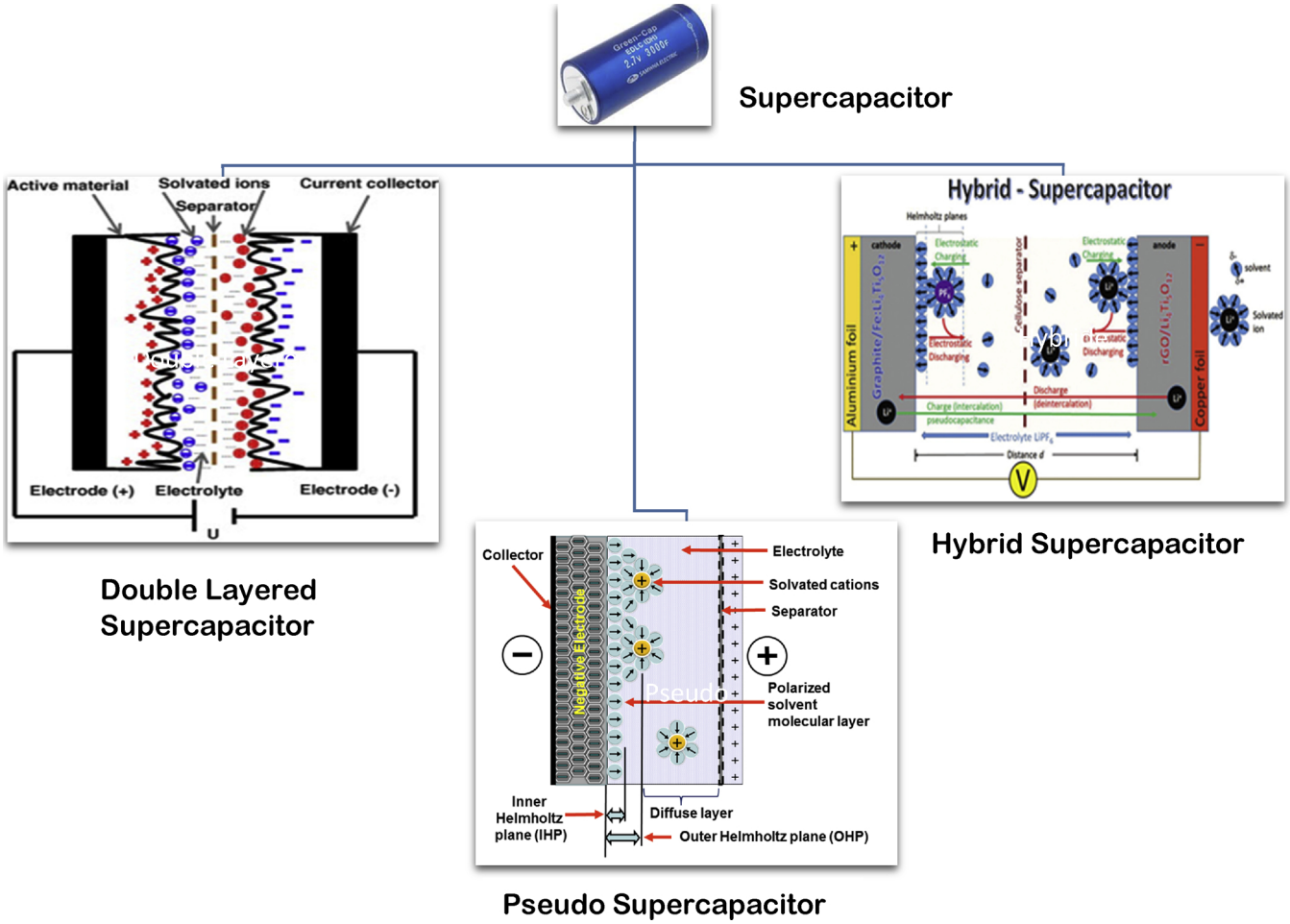

Fig. 3. Classification of supercapacitors based on electrode materials.

Fig. 4. Commercial supercapacitors as (a) EDLCs, (b) & (c) Pseudocapacitors, (d) & (e) Hybrid supercapacitors.

supercapacitors and (iii) Pseudo supercapacitors. Electrochemical double layer capacitors can be divided in 3 types i.e. activated carbon, carbon aerogels and carbon nanotubes. Hybrid capacitors also can be divided in 3 groups as asymmetric hybrid, battery type hybrid and composite hybrid. Similarly pseudo capacitors can be divided in 2 categories as conducting polymers and metal oxides.

2.1. Electric double-layer capacitors

The electric double-layer capacitor (EDLC) has been considered as a promising high-power energy source for digital communication devices and electric vehicles. The advantageous features of the EDLC are its better rate capability and longer cycle life as compared to modern secondary batteries. EDLC utilizes the double layer formed at the electrode/electrolyte interface where electric charges are accumulated on the electrode surfaces and ions of opposite charge are arranged in the electrolyte side. EDLC electrode materials should thus have a large surface area for charge accumulation and should have an appropriate pore structure for electrolyte wetting and rapid ionic motion. At present, activated carbons or molecular-sieving carbons are used as the EDLC electrode materials. Even if these conventional carbons have a large surface area, their EDLC application is rather limited because they contain pores ranging from micropores (< 2 nm dia) to macropores and the pores are randomly connected [34]. The micropores are not easily wetted by electrolytes, and the exposed surface in micropores may not be utilized for charge storage. Moreover, even in the situation wherein the micropores are wetted by the electrolyte, ionic motion in such small pores may be so slow that the high rate capability, which is one of the advantages of EDLCs, may not be realized [34]. Both charge storage and rate capability are further limited if the pores are randomly connected. The blind or isolated pores may not be wetted by electrolytes and irregular pore connection makes ionic motion difficult [35,36]. Therefore, high-surface-area carbon materials containing regularly interconnected mesopores (> 2 nm) are highly desirable for the EDLC electrode [37].

Double-layer capacitance – electrostatic storage of the electrical energy achieved by separation of charge in a Helmholtz double layer at the interface between the surface of a conductor electrode and an electrolytic solution electrolyte. The separation of charge distance in a double-layer is on the order of a few Ångströms (0.3–0.8 nm) and is static in origin [38]. Helmholtz laid the theoretical foundations of the double layer phenomenon. It is used in every electrochemical capacitor to store electrical energy. When Helmholtz first coined the phrase “double layer” in 1853, he envisioned two layers of charge at the interface between two dissimilar metals. Later, in 1879, he compared this metal/metal interface with a metal/aqueous solution interface [39]. In this model, the interface consisted of a layer of electrons at the surface of the electrode and a monolayer of ions in the electrolyte. Eq. 2 shows the phenomenon of polarization and the formation of double layer capacitance C.

More specifically, commercial EDLCs in which energy storage predominant is achieved by double-layer capacitance, energy is stored by forming an electrical double layer of electrolyte ions on the surface of conductive electrodes. Since EDLCs are not limited by the electrochemical charge transfer kinetics of batteries, it can charge and discharge at a lot higher rate with lifetimes of more than 1 million cycles [40]. Commercial EDLCs are based on two symmetric electrodes impregnated with electrolytes comprising tetraethyl ammonium tetrafluoroborate salts in organic solvents. Current EDLC with organic electrolytes operates at 2.7 V, reach energy densities around 5–8 W h/kg and 7–10 W h/l. The EDLC energy density is determined by operating voltage and the specific capacitance (farad/gram or farad/cm3) of the electrode/electrolyte system. The specific capacitance is related to the Specific Surface Area (SSA) accessible by the electrolyte, its interfacial double-layer capacitance, and the electrode material density.

The use of the high specific surface area blocking and electronically conducting electrode enable to achieve the high capacitance by charging the double layer. The attractive candidate that fulfills this criterion

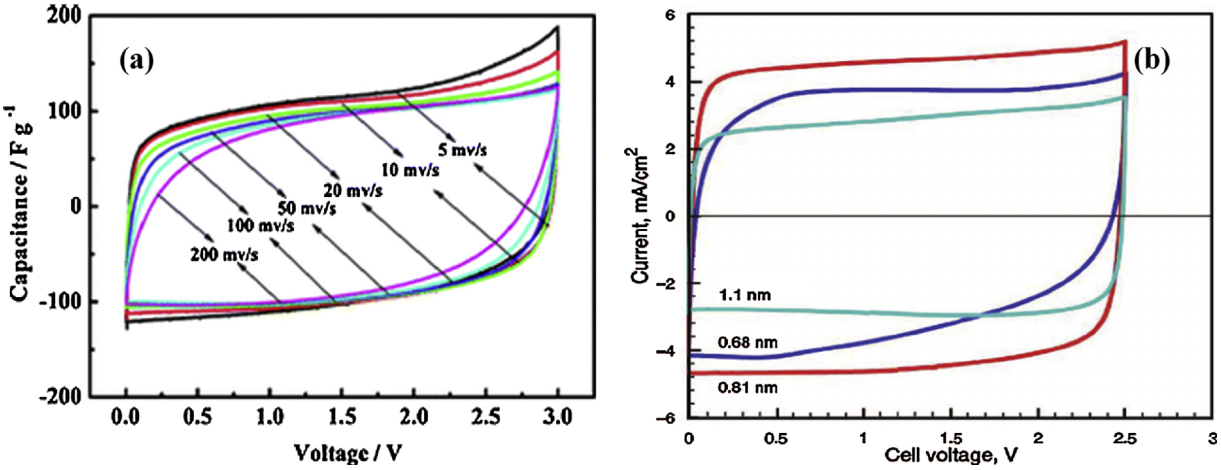

Fig. 5. Cyclic voltammetry of EDLCs at different (a) scan rates [45] and (b) current density [46].

is graphitic carbon used for the application. The properties include high conductivity electrochemical stability and open porosity [41]. The most widely used materials are activated carbons due to the high SSA and moderate cost. The examples are activated template and carbide-derived carbons, carbon fibers, carbon fabrics fibers, nanotubes [42], onions [43] and nano-horns [44] etc.

The double layer capacitance is 150-300 Fg^{-1} in aqueous electrolytes but the values declines in organic electrolytes to 100-120 Fg^{-1} at lower cell voltage as the electrolyte voltage window. is limited by water decomposition. Fig. 5 displays cyclic voltammetry (CV) of (a) MCNWNT in 1 M NEt_4BF_4-PC electrolyte at 5-200 mVs^{-1} scan rate and (b) TiC-CDCs in PYR_{14}-TFSI electrolyte at 5 mVs^{-1} scan rates in EDLC. The rectangular curve is characteristic of the EDLC charge storage mechanism followed by the double layer capacitance mechanism

$$I = C \times dV/dt \quad (6)$$

where I = current, C is double layer capacitance dV/ dt is potential scan rate. The rectangular shape CV curve at constant C shows that the at given scan rate the value of I is constant

A decreased capacitance (50-80 Fg^{-1}) is observed in the case of untreated carbon nanotubes [47] or nanofibers as compared to the activated carbon in an organic electrolyte. This value can be increased up to 100 Fg^{-1} by introducing oxygen groups to the substrates, but it affects cyclability. An appreciable capacitance is provided by activated carbon fabrics as possess similar SSA but are expensive. Graphene-based platelets with mesoporous spacer material is a promising structure for increasing the SSA of the electrolyte [4]. The improved cycle stability in EDLC capacitance is attained by pre-treating the carbon to remove moisture or other functional groups as explained by et al. P. Azais using NMR and x-ray photoelectron spectroscopic techniques [48]. The instability caused by the presence of oxygenated groups is also pointed out by the Pandolfo et. al in the review article resulting in the increased series resistance and deformation of the capacitance. Fig. 4 presents various commercial EDLCs. Energy capacitor system (ECaSS) connected an EDLC with power-electronics devices is useful for the compensation of fluctuating power since one is capable of controlling both active and reactive power simultaneously [49].

2.2. Pseudocapacitors

Pseudocapacitor is another type of supercapacitor, which is between a battery and an electric double layer capacitor. It also consists of two electrodes separated by an electrolyte. It has a chemical reaction at the electrode the electrical charge storage is stored electrostatically with no interaction between the electrode and the ions. Pseudocapacitance is accompanied by an electron charge-transfer between electrolyte and electrode coming from a de-solvated and adsorbed ion. One electron per charge unit is involved. The adsorbed ion has no chemical reaction with the atoms of the electrode (no chemical bonds arise) [50] since only a charge-transfer take place.

Chemical process involves charge transfer by means of reduction-oxidation (redox) reactions. While the charge transfer is like that in a battery, transfer rates are higher because of the use of thinner redox material on the electrode or lower penetration of the ions from the electrolyte into the structure. Because of multiple processes acting to store charge, the capacitance values are higher in Pseudocapacitors.

Pseudocapacitance was discovered by Conway, Birss, Wojtowicz, and Kozlowska in 1975, collaboration with Craig of Continental Group Inc. [51,52]. Research is still ongoing towards identifying materials and electrochemical characteristics that can render high energy density at faster charge-discharge rates. Electrodes' ability to produce pseudocapacitance strongly depends on the electrode materials' chemical affinity to the ions adsorbed on the electrode surface as well as on the electrode pore structure and dimension. To date, transition metal oxides have displayed pseudocapacitive behavior with high specific capacitance and multiple oxidation states that gains them a favor for capacitive application [53,54]. Another approach uses electron-conducting polymers as pseudocapacitive material. Although mechanically weak, conductive polymers have high conductivity, resulting in a low ESR and a relatively high capacitance. Such conducting polymers include polyaniline, polythiophene, polypyrrole, and polyacetylene [55]. Such electrodes also employ electrochemical doping or de-doping of the polymers with anions and cations. Electrodes made from or coated with conductive polymers are cost comparable to carbon electrodes. Conducting polymer electrodes generally suffer from limited cycling stability [56]. However, polyacene electrodes provide up to 10,000 cycles, much better than batteries. Fig. 4 (b) and (c) exhibits various commercial pseudocapacitors.

Pseudocapacitance is characterized by two-dimensional or near two-dimensional processes in storing charge. Fig. 6 shows three different mechanisms contribute towards pseudocapacitance: (a) underpotential deposition, (b) redox pseudocapacitance and (c) intercalation pseudocapacitance [27]. Underpotential Deposition occurs at potentials positive with respect to the Nernst potential. The deposition of a metal on to the electrode surface of another metal is at a reduction potential higher than that when it is deposited onto itself. The thickness of the deposit does not normally exceed a monolayer. The fractional surface coverage occurs over a continuous range of potentials. An example of Underpotential Deposition is the electrosorption of hydrogen on platinum or lead on gold. The chemical reaction involving the deposition of lead on gold can be represented [53] as [20]: The reaction rates and

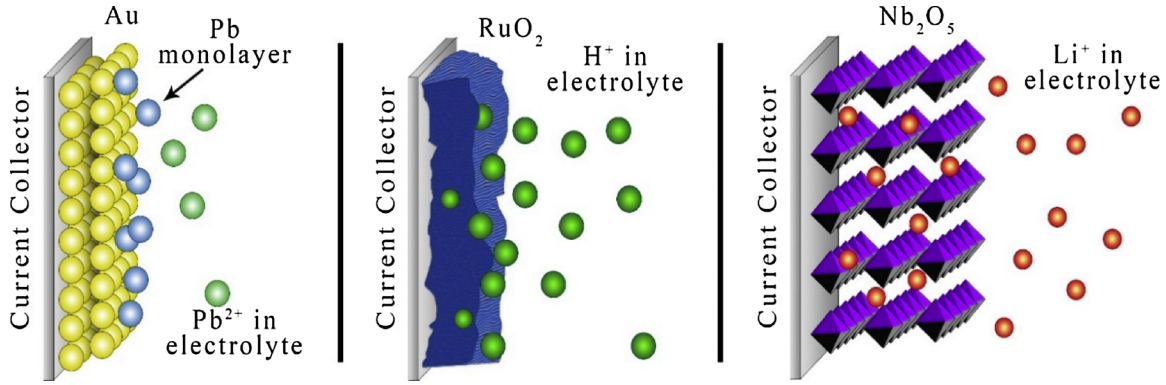

Fig. 6. Different types of reversible redox mechanisms that give rise to pseudocapacitance: (a) underpotential deposition, (b) redox pseudocapacitance and (c) intercalation pseudocapacitance [27].

the resulting surface structures depend on the nature and concentration of anions. Depending on the level of lattice match between the adsorbate and substrate, the structures of the substrate and the grown layers are in proportion [52,57].

The charge transfer between electrode and electrolyte occurs by means of redox reactions in the case of redox pseudocapacitance and hence Faradaic in nature. Redox reactions mean reduction-oxidation reactions. Both result in the change of oxidation state of the species involved. Reduction occurs when electrons are accepted, and the oxidation state gets lowered. Oxidation indicates release of electrons and an increase in the oxidation state. For the case of ruthenium oxide (hydrated) which was first discovered to exhibit pseudocapacitance, redox occurred by accepting protons from the electrolyte and releasing them back to the electrolyte. While accepting protons it also takes in electrons and changes its oxidation state from +4 to +3 [58].

Insertion of cations into the bulk lattice of a solid electrode is termed intercalation. There should be an appropriate number of electrons transferred to the host during insertion to maintain the electrical neutrality of the electrode. Insertion is limited by the ability of the ion to diffuse through the electrode material. Current flow in this case at a given voltage varies with the square root of the sweep rate [59]. Fig. 7 shows cyclic voltammogram and charge-discharge curves of a pseudocapacitor electrode material.

3. Materials

Material selection is very important for supercapacitors. Various materials are used as an electrode (anode & cathode) and electrolyte in supercapacitors system. The properties of supercapacitors come from the interaction of their internal materials. Especially, the combination of electrode material and type of electrolyte determine the functionality and thermal and electrical characteristics of the capacitors.

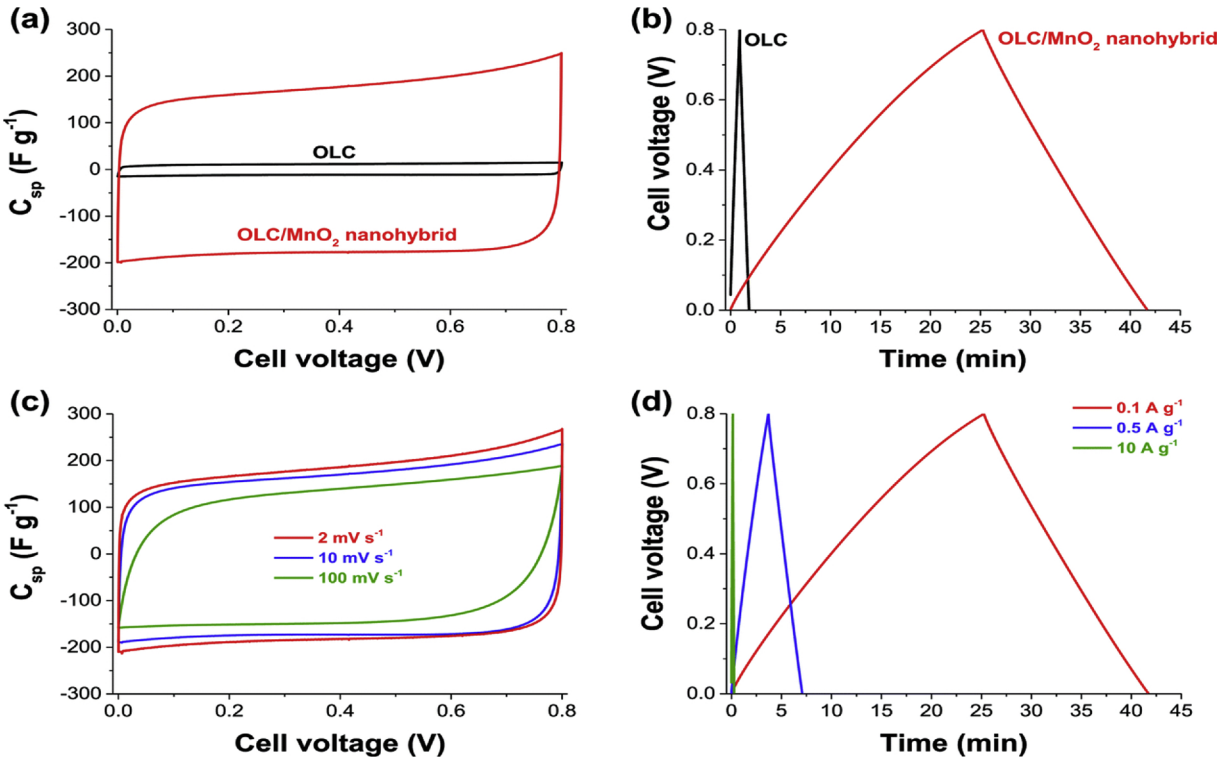

Fig. 7. Nickel foam based 2-electrode (symmetric) configuration: (a) comparative cyclic voltammogram for OLC and OLC/MnO_2 at 5 mV s^{-1}, (b) comparative galvanostatic charge–discharge curves for OLC and OLC/MnO_2 at 0.1 Ag^{-1}, (c) CVs at different scan rates for [60].

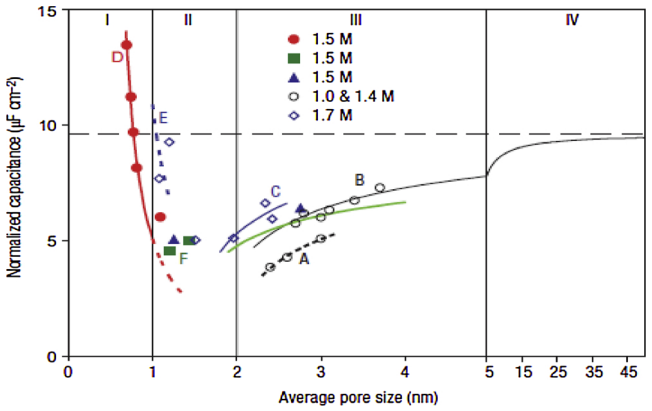

Fig. 8. Specific capacitance normalized by SSA as a function of pore size for different carbon samples.

3.1. Electrode

Electrodes for any energy storage and conversion system must have good conductivity, high-temperature stability, long-term chemical stability, high corrosion resistance, high surface areas per unit volume and mass, environmental friendliness and low cost. Supercapacitor electrodes are generally thin coatings applied and electrically connected to a conductive, metallic current collector. These are typically made of a porous, spongy material with an extraordinarily high specific surface area. Additionally, the ability of the electrode material to perform faradaic charge transfers enhances the total capacitance. Electrode material fabrication is very important to get high-performance supercapacitor [61,62]. As an example, a novel colloidal self-assembly method was used to fabricate graphene-MWCNT-polypyrrole nanofibers composite electrode materials [63–68]. Also, chemical deposition, electrodeposition, electrophoretic deposition, hydrothermal, noncovalent functionalization, electrochromic, liquid-phase deposition (LPD), linearized augmented-plane-wave (LAPW) are various promising methods to fabricate electrode materials for supercapacitors [69–72]. With respect to electrode materials, there are the following categories: carbon-based, metal oxides based, perovskite-based and conducting polymer based. The detailed descriptions of the various systems will be discussed in the following sections. For each type, the present status is summarized first and then prospects for future development are discussed. There have been many excellent reviews focusing on the electrode materials reported during the past several years [53,73–77].

3.1.1. Carbon-based

The most commonly used electrode material for supercapacitors is carbon. For high availability, established industrial production processes and low cost, various carbon-based materials are widely used in many applications for supercapacitors [78]. Carbon electrodes can be manufactured as several forms of 1D to 3D structure such as foams, fibers, and nanotubes. One might expect the specific capacitance to be directly proportional to the carbon electrode's surface area, however, this is not always the case. Often, a type of carbon with a lower surface area will have a higher specific capacitance than a type with a larger surface area [77].

Activated carbon (AC) is used as active electrode material for supercapacitor due to relatively low cost and high specific surface area (SSA) around 1000-2000 $m^2 g^{-1}$ [40,73,79]. It is obtained from carbon-rich organic precursors by carbonization (heat treatment) in an inert atmosphere, with subsequent oxidation in CO_2, water vapor or KOH to increase the SSA and pore volume. Natural or synthetic materials like coconut shells, wood pitch, coal or polymers can be used as precursors respectively. A network of micropores (< 2 nm), mesopores (2–50 nm), and macropores (< 50 nm) was created in the bulk of carbon grains by activation [80]. The broad distribution of pore size is characteristic of the porous structure of carbon. Higher temperature or longer activation time leads to larger pore size. To increase the pore volume by SSA preliminary research was focused on the refining the activation process of the activated carbon. But the capacitance increase was not very appreciable even for the most porous samples. A nonlinear relationship between SSA and capacitance is understandable from various activated carbons with different pore sizes in various electrolytes [81–83]. Several investigations reveal that the pores smaller than 0.5 nm were not approachable by the hydrated ions [84], even 1 nm pores are not accessible mainly in case of organic electrolytes as the solvated ion has a larger size than 1 nm [85]. The new findings are in accord with the previous investigations where the removal of the solvation shell [86] sheath needs several kilojoules per mole in case of water molecules [87]. To improve the energy density and power capability a pore size distribution in the range of 2–5 nm was considered appropriate as it is larger than the size of two solvated ions. The moderate improvement is depicted by the gravimetric capacitance in the range of 100-120 Fg^{-1} in organic solvents and 150-200 Fg^{-1} in aqueous electrolytes [88,89] and ascribed to improve ionic mass transport inside mesopores. It is reported that micropores show better performance in comparison to the fine-tuned mesoporous carbon. Salitra et. al. suggested that partial desolvation can help in better capacitance by accessing the small pores (< 2 nm) [90]. Mesoporous carbon having small pores exhibited a high capacitance, suggesting that partial ion desolvation might be the reason for capacitance [91–93]. Microporous carbons (< 1.5 nm) in organic electrolytes showed (120Fg^{-1} and 80 Fcm^{-3}) contradicting the solvated ion adsorption theory [94,95]. Raymond-Pinero et al. found the same capacitance results using activated microporous coal-based carbon materials of 0.8 and 0.7 pore sizes in organic or aqueous electrolytes [96]. The use of the carbide-derived carbons (CDCs) resulted in a promising rise in capacitance by smaller pores than solvated ion size [97–101]. The porous carbons are obtained by extraction of metals from carbides by etching halogen at high temperature are

$$TiC + 2Cl_2 \rightarrow TiCl_4 + C \quad (7)$$

During the above process Ti is leached out of TiC carbon atoms adopt amorphous or random organization by sp^2 bonding linkage the pore size can be controlled by chlorination temperature and other parameters. A contracted uni-modal pore size distribution can be achieved accordingly in (0.6–1.1 nm) range, with controlled pore size up to sub-angstrom level accuracy [102].

A theoretical analysis published by Huang et al. proposed two approaches depending on pore size for the capacitive behavior. The pores of mesoporous carbon larger than 2 nm model describing the charge of the double layer were used [103].

$$C/A = \varepsilon_0 \varepsilon_r / b \ln (b/b–d) \quad (8)$$

Where b is the pore radius and d is the distance of approach of the ion to the carbon surface. Fig. 8 shows the mesoporous range (zone III) were fitted with Eq. 8. For micropores (< 1 nm) it was assumed that ions enter a cylindrical pore and line up, thus forming the electric wire in a cylinder

$$C/A = \varepsilon_0 \varepsilon_r / b \ln (b/a^o) \quad (9)$$

where a^o is the effective diameter of the desolated ion. This model matches with the normalized capacitance change versus pore size (zone I Fig. 9). This research suggests that the removal of the solvation shell is mainly by the ion's entry in the micropores. Eq. 8 suggests that ionic radius a^o is close to the bare ion size, mean full desolvation can happen. The interaction of CDCs with the solvent-free electrolyte [EMI^+, $TFSI^-$] where both ions have a maximum size of about 0.7 nm pore size at 60 °C showed maximum capacitance for 0.7 nm samples. This may be due to single ion per pore produces the maximum capacitance, proposing that ions cannot be absorbed on both pore surfaces, in contrast to the

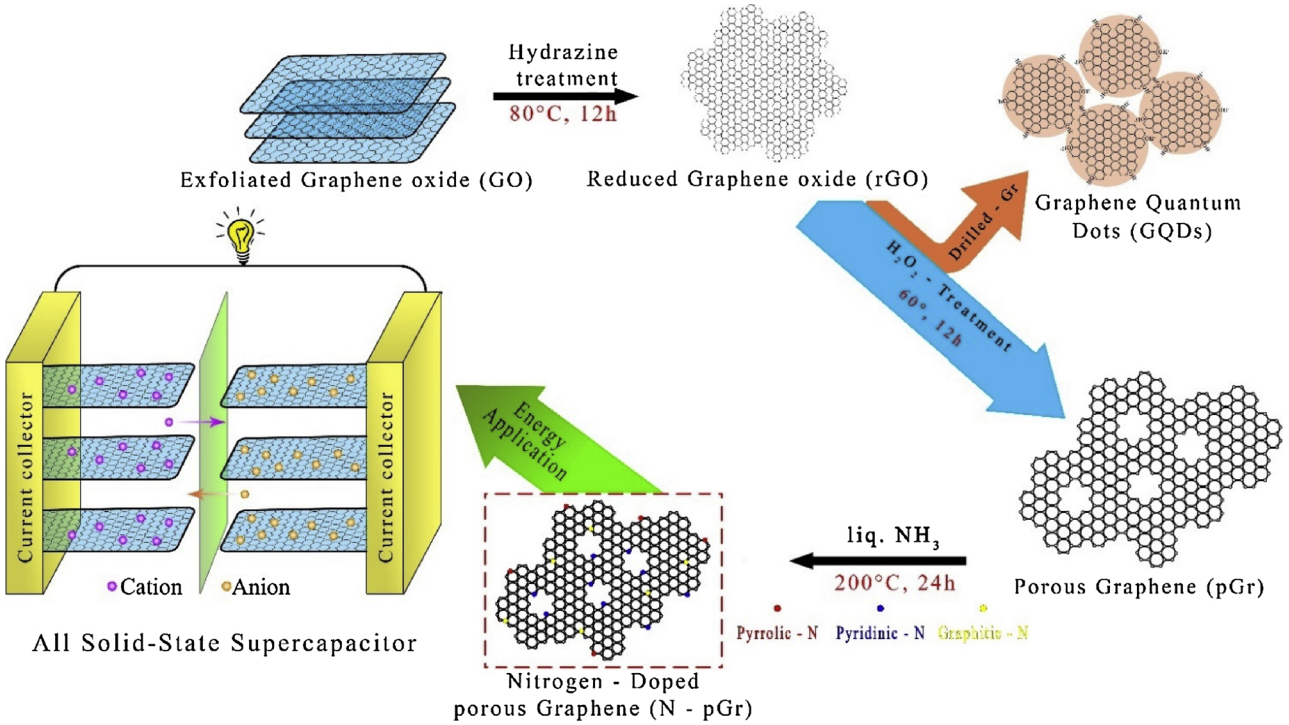

Fig. 9. Schematic illustration for the synthesis of porous graphene [105,106].

traditional supercapacitors. Carbon hollow fibers as promising material were reported to achieve 287 Fg^{-1} at 50 mAg^{-1} with capacitance retention of 86.4% at 1Ag^{-1} [104].

Carbide-derived carbons (CDCs) with Titanium was shown to have the highest gravimetric capacitance, up to 220 Fg^{-1} in KOH and 120Fg^{-1} in organic electrolyte whereas SiC-CDC has the highest volumetric capacitance 126 Fcm^{-3} in KOH and 72 Fcm^{-3} in organic electrolyte [107]. Carbon nanotubes (CNTs) were used as supercapacitor electrode materials with a specific capacitance of 115.7 Fg-1 in 1 M H_2SO_4 and good electrochemical stability [108].

Graphene is the monolayer of graphite, which can be prepared by several techniques. Geim et al. prepared graphene from graphite and demonstrated an experimental method to prepare a single layer of graphite with a thickness in the atomic scale, named as graphene. Fig. 9 presents the schematic diagram of the synthesis process of porous graphene. Graphene oxide (GO) is another important member of the graphene-graphite family, which is considered as derivatives of graphene. They that can be readily made from graphite, exhibit the layered structure and the surface related properties [109,110]. Graphene-based supercapacitors were reported with a specific capacitance of 75Fg^{-1} and energy density of 31.9 $Whkg^{-1}$ with ionic liquid electrolytes [111]. Zhang et al. reported a method to prepare porous 3D graphene-based materials which produce 92 Fcm^{-3} volumetric capacitance, 231 Fg^{-1} specific gravimetric capacitance and 98 $Whkg^{-1}$ energy density [112]. Lee et al. fabricated vertically aligned graphene which produces 171 Fcm^{-3} volumetric and 1.83 fcm^{-2} areal capacitance [113]. Tho et al. reported that a maximum specific capacitance of 199 Fg^{-1} was measured in KOH electrolyte is achieved by using GO [114]. Reduced graphene with low agglomeration reached a maximum specific capacitance of 205 Fg^{-1} in aqueous electrolyte exhibiting an energy density of 28.5 $Whkg^{-1}$ [115].

Recently Y. Yang et al. reported graphene-based materials as potential perspective electrode materials for energy conversion and storage for future research. He compiled as highest specific capacitance 843 Fg^{-1}, highest energy density 155.6 $Whkg^{-1}$ and highest power density 400 kW kg^{-1} as reported all potential GBMs [116]. At the same time period Q. Ke et al. summarizes recent development on graphene-based materials for supercapacitor electrodes, based on their macrostructural complexity, i.e., zero-dimensional (0D) (e.g. free-standing graphene dots and particles), one-dimensional (1D) (e.g. fiber-type and yarn-type structures), two dimensional (2D) (e.g. graphene and graphene-based nanocomposite films), and three-dimensional (3D) (e.g. graphene foam and hydrogel-based nanocomposites) [117]. Table 2 shows the various carbon-based materials with electrochemical performances.

The application of SCs calls for an electrode with a structure that allows for the long and continuous transfer channels of electrons and short diffusion distances for the ions of the electrolytes, stimulating the development of fabricating carbon-based materials as 3D graphene and graphene and CNT hybrids. The capacitance performance of CNT/graphene-based nanomaterials with high chemical stability in high voltage is encouraging, since their hexahedral surface configuration and mesopores in large amount have improved the power density of the electrode significantly, while the energy density also increases because it's proportional to the square of the voltage.

3.1.2. Metal oxide based

Metal-oxides present an attractive alternative as an electrode material for high energy and high power supercapacitor because of high specific capacitance and conductivity, low resistance, possibly making it easier to construct high-energy, high-power supercapacitors [17]. A variety of metal oxides have been employed as an electrode in supercapacitors. These include of RuO_2, MnO_2, NiO, SnO_2, In_2O_3, IrO_2, MoO_x, Co_2O_3, V_2O_5, Fe_2O_3, Bi_2O_3, $BiFeO_3$ etc. Fig. 10 (a) shows the morphologies of various metal oxide films.

Ruthenium IV Oxide was the first material to exhibit highest specific capacitance), high proton conductivity, good thermal stability and electrochemical reversibility, high rate capability, wide potential window, and long cycle life [129–132] and it has a specific capacitance of 720 to 1340 Fg^{-1} in water. It has three oxidation states within a potential of 1.2 V. Limited occurrence and high costs inhibit further exploration of the material [53]. The maximum Sc of over 768 Fg^{-1} has been obtained in $RuO_2.xH_2O$ [133]. Because of the high cost, RuO_2 was combined with other low-cost materials. It is reported that with RuO_2-

Table 2
Carbon based electrode materials with electrochemical performances.

Electrode	Electrolyte	Characterization Method	E_{max} (Wh/kg)	P at E_{max} (W/kg)	Max Specific Capacitance (F/g)	Current density (A/g)	Scanning rate (mV/s)	Retention with cycle	Reference
Self-stacked solvated graphene (SSG)	PVA-H_2SO_4	Facile vacuum filtration	8.01	5.97 k	245	1	100	83% @10,000	[118]
Surfactant modified rGO with Triblock copolymer pluronic F127	6 M KOH	Hydrothermal and thermal annealing procedures			210	1	1	95.6% @1000	[119]
CNTs 25 wt% with activated GO	1 M KOH	Coulombic interaction	110.6	400k	199	0.5	40	98.2% @10,000	[114]
CNTs with reduced GO	1 M EMI-TFSI	Modified Hummers method	155.6		280	0.3	10.3	57.8% @1000	[120]
Activated Carbon with Hydrothermally reduced GO	6 M KOH	Hydrothermal	22.3	33.2	210		1	94.7% @5000	[121]
Carbon fiber with electrochemically reduced GO	1 M Na_2SO_4	Electrochemical deposition	8.5 mW/cm2	21.4 μWh/cm2	22.6 μF/cm		10	95.5% @5000	[122]
Porous carbon with Pyrolysis GO	6 M KOH	Situ polymerization	11.3 Wh/L	45W/L	481	0.5	500	97.2% @5000	[123]
Holey Graphene (HGF)	Polyvinyl alcohol (PVA) gel	Reduction			298			87% @ 10,000	[124]
Multi-redox anthrauinone derivative alizarin (AZ) with 3D self-assembled graphene hydrogel (SGHs)	1 M H_2SO_4	Hydrothermal	18.2	700	350	1		61%	[125]
Flexible graphene paper with carbon black nanoparticles		Vacuum filtration			138	10	10	96.15% @2000	[126]

SnO_2 composite electrode showed Sc of 710 Fg^{-1} in KOH electrolyte [134] and RuO_2-TiO_2 showed 534 Fg^{-1} [135]. Further, RuO_2 has been also co-deposited with InO_2 and V_2O_5 using sol-gel and dip coating methods. Fig. 10(a) shows the morphologies of various transition metal oxide thin films [99] and Fig. 10(b) shows the cyclic voltammograms of a MnOx based electrode material [100].

After RuO_2, most attention had focused on manganese oxide (MnO_2) as electrode material due to lower cost, lower toxicity, environmental safety and theoretical high capacitance (1100-1300 Fg^{-1}). Various synthesis methods, such as sol-gel, dip or drop coating, electrochemical deposition etc.; were used to prepare MnO_2 thin film. Fig. 10 (b) exhibits the cyclic voltammograms of MnO_x based electrode 1 M Na_2SO_4 at a scan rate of 50 mV s^{-1}. It is reported that, MnO_2 showed a Sc of 600-700 Fg^{-1} in 1 M Na_2SO_4 [136], 195-275 Fg^{-1} in 2 M KCl, 310 Fg^{-1} in 2 M $(NH_4)_2SO_4$ [137] and 720 Fg^{-1} in $LiClO_4$ aqueous solution electrolyte [138]. Recent studies reported that MnO_2 coated MWCNT composites could be prepared N-doped activated carbon (N-AC) as a sacrificial template [139,140]. The problem of MWCNT degradation in the reaction with $KMnO_4$ has been avoided by the N-AC layer. This process offers the advantages of the small size of MnO_2 nanoparticles, the fibrous microstructure of composite and good electrical contacts. The result shows high specific capacitance of 311.7 Fg^{-1} (6.29 Fcm^{-2}) at a high mass loading of 20 mg cm^{-2} and in the asymmetric device of Na_2SO_4 electrolyte, the energy density is 26.4 $mWhg^{-1}$ with a power density of 1.7 Wg^{-1}.

Nickel cobaltite has displayed very high specific capacitances in the range of 330 to 2680 Fg^{-1}. The existence of multiple oxidation states for Nickel and Cobalt and high electrical conductivity boosts the capacitance. Moreover, the ease of availability of both Nickel and Cobalt makes the substance more accessible [141]. Nanowire arrays of nickel cobaltite prepared by a hydrothermal process exhibit the highest reported capacitance obtained at a current density of $2Ag^{-1}$ in PVA-KOH polymer gel as the electrolyte. The arrays were grown on Ni foam and had a mass loading of 3 mg cm^{-2} [142]. Nickel Cobaltite aerogels prepared through an epoxide-driven sol-gel procedure have a specific capacitance of 1400 Fg^{-1} at a scan rate of 25 mVs^{-1} in a potential window of 0.5 V in 1 M NaOH solution. The mass loading was at 0.4 mg cm^{-2}. Electrodeposition is also utilized in the synthesis of Nickel Cobaltite [54]. Cobalt Hydroxide synthesized by means of electrodeposition as an ordered mesoporous film on foamed Nickel mesh has a specific capacitance of 2646 Fg^{-1}. The film studied under electron microscopes exhibits a surface with interlaced nano-sheet like appearance, pores of nanometer dimension and a regular nanostructure with extended periodicity [143]. Amorphous Nickel Hydroxide nano-spheres deposited on a graphite rod in 1 M potassium hydroxide and cycled at current densities of 20-70 Ag^{-1} show specific capacitances between 1868 to 1330 Fg^{-1}. Irregular surfaces and amorphous character render such high capacitance [144].

For intercalative pseudocapacitance properties $Co(OH)_2$, Co_3O_4 and CoO_x are promising electrode materials for supercapacitors. It was reported that a Sc of 280 Fg^{-1} was obtained by $Co(OH)_2$ [145], 291 Fg^{-1} by CoO_x xerogel [146] and 730 Fg^{-1} by (CO + Ni)$(OH)_2.nH_2O$ [147]. Zhao et al. obtained a Sc of 578 Fg^{-1} in 3% KOH electrolyte [148]. Wu et al. used nickel foil and graphite obtaining Sc of 135 and 195 Fg^{-1} respectively [149]. A maximum Sc value of 840 Fg^{-1} was obtained with electrochemically deposited nickel and cobalt mixed oxide onto CNT film substrate [150]. Recently it is reported that Ni and Co- based oxides/hydroxides has been termed as battery-type faradic electrode materials based on their electrochemical behavior in aqueous electrolytes. The capacitance for these materials was not constant over the whole potential window in cyclic voltammogram test [22,151–154]. It is confusing to use these materials as pseudocapacitive, that might exhibit high-rate capability, but with the electrochemical signature of a 'battery' electrode.

Due to high conductivity, tin oxide (SnO_x) is used for electrode materials in supercapacitor. It was reported that a Sc of 285 Fg^{-1} was

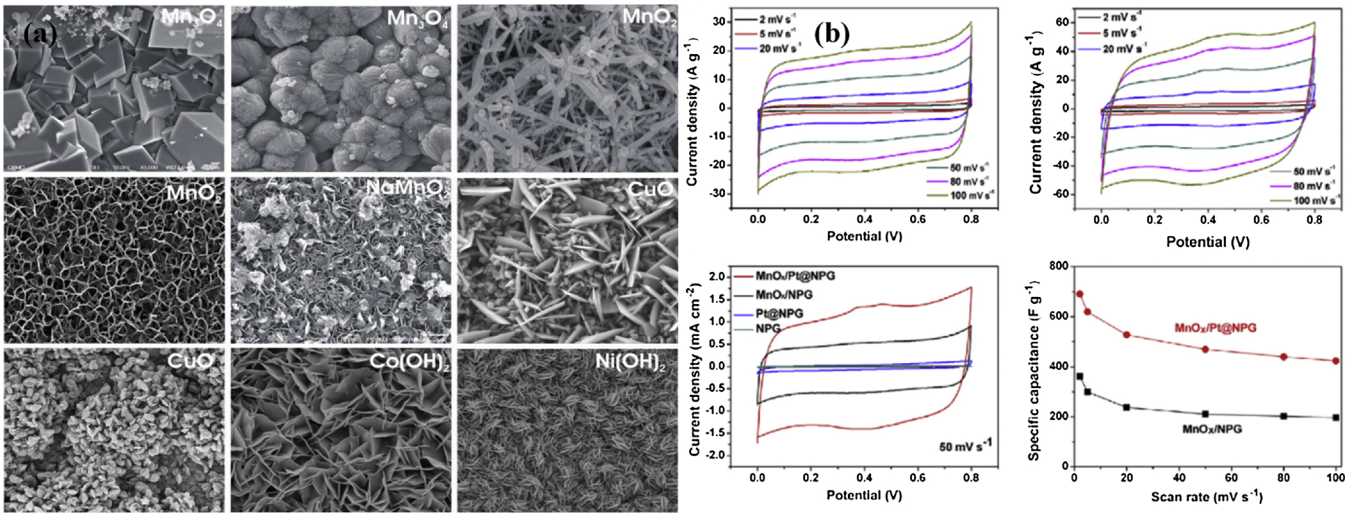

Fig. 10. (a) Morphologies of various transition metal oxide thin films [127] and (b) Cyclic voltammograms of a MnO_x based electrode material [128].

Table 3
Metal oxide-based electrode materials with electrochemical performances.

Electrode	Electrolyte	Characterization Method	E_{max} (Wh/kg)	P at E_{max} (W/kg)	Max Specific Capacitance (F/g)	Current density (A/g)	Scanning rate (mV/s)	Retention with cycle	Reference
RuO_2	1 M H_2SO_4	Electrophoretic deposition	25	21	734	10	1	91% @200	[166]
MnO_2	0.1 M Na_2SO_4	Sol-gel dip coating			698		50	73.6% @1500	[167]
$Ca_3Co_2O_6$		Solid-state calcination and co-precipitation			563		5		[168]
SnO_2	0.1 M Na_2SO_4	Sol-gel			285	0.3 mA/cm2	10	88% @1000	[155]
$Co(OH)_2$nanowires	6 M KOH	Hydrothermal	13.6	153	358	0.5	1	86.3% @5000	[169]
In_2O_3	1 M Na_2SO_3	Potentiodynamic			190	3	10	@1000	[160]
$Al_{0.2}Cu_{0.4}Co_{0.4}Fe_2O_4$		Sol-gel		0.27	548		100		[170]
Bi_2O_3	1 M NaOH	Electrodeposition			98		100	@1000	[161]
V_2O_5	2 M KCl	Solvothermal			350			@100	[158]
Fe_3O_4	1 M Na_2SO_3	Wet chemical			170		2		[162]
	1 M Na_2SO_4				25				
	1 M KOH				3				
$NiFe_2O_4$	Na_2SO_3	Modified chemical			354	5		@1000	[165]
					95	200			
$MnFe_2O_4$	1 M NaCl	Co-precipitation	7.6	10	100	0.5	20		[163] [164],
Ti (RhOx + Co_3O_4)	0.5 M H_2SO_4	Thermal decomposition			500-800 @ 20-60 mol% RhO_x		20	@100	[171]

obtained in 0.1 Na_2SO_4 electrolyte [155]. Kuo and Wu reported that a Sc of 930 Fg^{-1} was obtained with supercapacitor containing sol-gel SnO_2 and electroplated RuO_2 [156]. In the non-aqueous electrolyte category, Vanadium oxide aerogels immobilized on a sticky carbon electrode in 1 M Lithium perchlorate in propylene carbonate gave specific capacitance of 2150 Fg^{-1}. The aerogels were prepared by ambient drying method. The drying was done with a low surface tension solvent at ambient pressure resulting in larger pores of 10–30 nm size range. Large pores combined with significant pore volume improved the probability of electrolyte penetration. Electron, ion and solvent transport are enhanced by the choice of the current collector and the aerogel morphology ensuring shorter diffusion lengths. It has ion incorporation like a battery and response of a capacitor [157].

Vanadium pentoxide (V_2O_5) plays an important role in the electrochemical supercapacitor. Lee and Goodenough reported with Sc of 350 Fg^{-1} in aqueous KCl [158]. In an organic electrolyte ($LiClO_4$ in propylene carbonate), the $V_2O_5.xH_2O$/CNT film electrode showed Sc of 910 Fg^{-1} at 10 mVs^{-1} of scan rate [159]. Indium oxide (In_2O_5) was used as electrolyte materials in supercapacitor and showed Sc of 190 Fg^{-1} at a scan rate of 10 mVs^{-1} in 1 M Na_2SO_3 electrolyte [160]. Polycrystalline monoclinic Bismuth oxide (Bi_2O_3) electrolyte showed a Sc of 98 Fg^{-1} in 1 M NaOH electrolyte [161]. Wang et al. reported that an Iron oxide (Fe_3O_4) thin film electrode exhibited Sc of 170 Fg^{-1} in aqueous 1 M Na_2SO_3 [162]. The capacitive current of magnetite electrode originates from the combination of EDLC and pseudo-capacitance that involves successive reduction of the specifically adsorbed sulfite anions. The bulk ferrites (MF_2O_4, where M = Mn, Ni, Co, or Fe) showed potential electrode candidate for supercapacitor. Kuo and Wu used MnFe2O4, which exhibited Sc of 100 Fg^{-1} and had high power delivery capabilities of 10 kW kg-1 [163,164] and Gunjakar used spinal $NiFe_2O_4$ films exhibited Sc of 354 Fg^{-1} at 5 mVs^{-1} [71,165]. Table 3 shows the different values obtained from different metal oxide thin film-based supercapacitors. The supercapacitors exhibited superior values compared to their bulk and composite electrode.

Metal oxide-based supercapacitors also exhibited superior values compared to their bulk and composite electrodes and for some oxide materials, are higher than the carbon and polymer-based electrode systems. Further, increase in energy density of supercapacitor is projected if the nanostructure of electrodes and surface faradaic charge-storage properties are combined. Considering that metal oxide-based supercapacitor technology is still in its infancy, future research and development should ultimately yield high-performance, low cost, and safe energy storage devices.

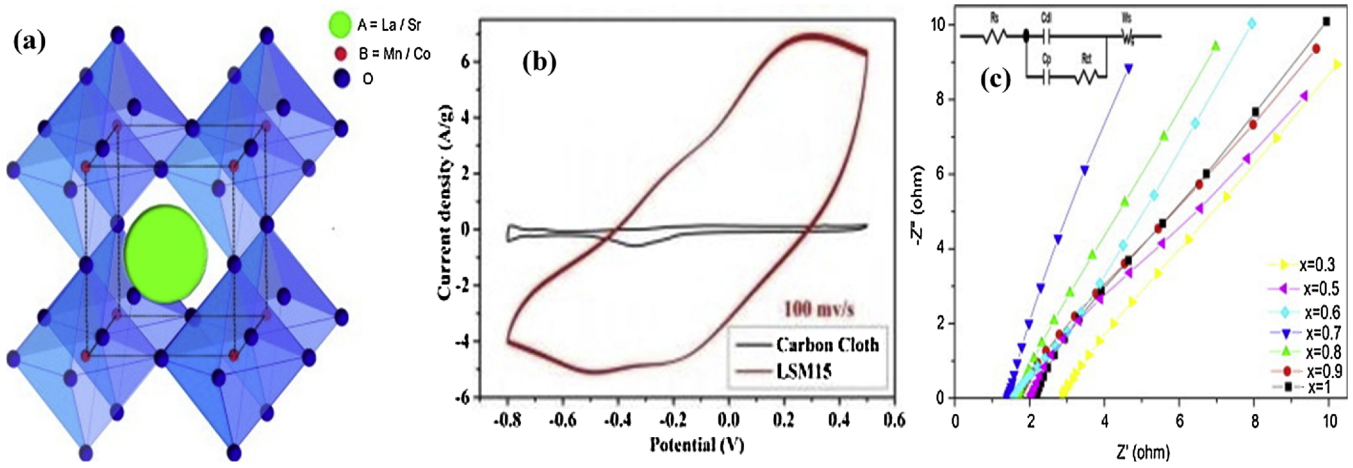

Fig. 11. (a) Idealized cubic ABO_3 perovskite structure, (b) Cyclic voltammograms (CVs) of $La_{0.85}Sr_{0.15}MnO_{3-\delta}$ in 1 M KOH at scan rate of 100 mVs^{-1} and (c) Nyquist plots of $La_xSr_{1-x}Co_{0.1}Mn_{0.9}O_{3-\delta}$ in 1 M KOH [173,174].

3.1.3. Perovskite based

Perovskite term is used when referring to a large group of compounds with a crystal structure resembling the minerals $CaTiO_3$, which is very stable and orthorhombic at high temperatures, was named after the Russian mineralogist Lev Perovski [172]. The general formula of perovskites is ABX_3, where A and B represent cations, and X is an anion. A-site cations are usually bigger and more electropositive in comparison to ones located at B-site, while the X site is commonly occupied by oxide or halide ions (O^{2-}, Cl^-, Br^-, F^-). Combination of the large oxide ion with a smaller radius metal ion gives a cubic close-packed crystal structure of ions along with interstitial metal ions. The possible use of ABO_3 structures as catalysts in the replacement of noble metals is an idea that has been proposed in the early 1990s, based on the mixed oxide-ion/electronic conductivity and the low cost of these materials. Fig. 11 shows the structure and performance of the perovskite supercapacitor electrode material [173].

The perovskite crystal structure is a combination of metal oxides. Perovskite-based materials exhibit high chemical stability and good electrochemistry performance. Due to its good performance perovskite-based electrode materials for supercapacitor. Garche et al. reported that $SrRuO_3$ showed a Sc of 10 Fg^{-1} in KOH electrolyte. Doping La on A-site the Sc value increase to 20-30 Fg^{-1} [175]. Wohlfahrt made the same electrode with a better result (270 Fg^{-1}) [176]. Lee et al. reported CO sensing characteristics of rGO/$GdInO_3$ nanocomposite by one step hydrothermal method showed high response at low temperature [177]. Atma et al. prepared $La_{1-x}Al_xFeO_3$ (x = 0, 0.3) as electrode made by chemical route in 1 M H_2SO_4 exhibited a Sc of 260 Fg^{-1} at 500 mVs^{-1} [178]. Jung and his coworker prepared (Na, K)NbO_3-$CaCu_3Ti_4O_{12}$ perovskite composite for supercapacitor with a maximum dielectric permittivity of 796 Fg^{-1} [179]. Han et al. prepared $BiFeO_3$ thin film electrode for electrochemical supercapacitor which showed a Sc of 81 Fg^{-1}, specific energy of 6.68 Jg^{-1} and specific power as 3.29 Wg^{-1} in aqueous NaOH [180]. Fig. 11 shows an idealized cubic ABO_3 perovskite structure (a), cyclic voltammograms (CVs) of $La_xSr_{1-x}Co_{0.1}Mn_{0.9}O_{3-\delta}$ in the different solutions at a sweep rate of 5 mVs^{-1} (b) and Nyquist plots of $La_xSr_{1-x}Co_{0.1}Mn_{0.9}O_{3-\delta}$ in 1 M KOH (c) [139].

Hwang and Kim reported $LaNiO_3$ nanofibers as electrode for supercapacitor with a Sc of ~160 Fg^{-1} at 10 mVs^{-1} [181]. Lin et al become successor on using perovskite electrode materials for supercapacitors. $La_xSr_{1-x}Cu_{0.1}Mn_{0.9}O_{3-}\delta$ ($0.3 \le x \le 1$) exhibited a Sc of 464 Fg^{-1} at 2 Ag^{-1} and maximum current density 64.5 $Whkg^{-1}$ at 2 kW kg^{-1} of power density [182]. Doping with Ni and Co the electrode exhibited a Sc of 719 Fg^{-1} and 747 Fg^{-1} [183,184]. Jie and Hao made $LaMnO_3$/graphene film by sol-gel with the spin-coating method. Mobin et al. developed nanocomposite rGO/$SrTiO_3$ electrode material with rapid electronic communications [185,186]. Yang et al. made promising lanthanum based perovskite electrode material in a different aqueous solution which showed good specific capacitance and excellent electrochemical behavior [187]. Liu and Shao et al developed $SrCo_{0.9}Nb_{0.1}O_{3-\delta}$ (SCN) as a novel anion-intercalated electrode material for supercapacitors, demonstrating a very high volumetric capacitance of about 2034.6 Fcm^{-3} [188]. Table 4 shows the different values obtained from different perovskite-based supercapacitors.

Perovskite based electrode materials were mainly combination of metal oxides. But due to the unique structure, this material has been used in supercapacitors application to get the better performance. The perovskite materials can achieve high capacitance through the anion-insertion mechanism, paving a new way for the development of supercapacitors with high energy and power density. The perovskite-based materials have potential as remarkable electrodes in the next-generation high-performance supercapacitors.

3.1.4. Conducting polymer based

Conducting polymer has high electric conductivity (10^4 Scm^{-1}). As expected for a capacitor, the typical cyclic voltammogram of a conducting polymer is not rectangular and exhibits a current peak at a redox potential of the polymer. Conducting polymers store and release charge through redox processes. When oxidation occurs (doping), ions are transferred to the polymer backbone. When reduction occurs (de-doping) the ions are released back into the solution. Charging in conducting polymer films, therefore, takes place throughout the bulk volume of the film, and not just on the surface as is the case with carbon. This offers the opportunity of achieving high levels of specific capacitance. Fig. 12 shows the different characteristics of PANI electrode for a supercapacitor application.

Polyaniline was first described by Henry Letheby in the mid-19th century, who investigated the electrochemical and chemical oxidation products of aniline in acidic media [192]. Due to its large theoretical capacitance, low cost and facial synthesis among conducting polymers, polyaniline (PANI) is the most widely used for the energy storage application, especially supercapacitors, either as a conducting agent or directly as an electroactive material. PANI morphology is very important in all solid-state cell in which the electroactive material is not soaked in the electrolyte to increase the electrode/electrolyte interface and increasing the electrochemically accessible surface area by forming porous PANI can also significantly improve the supercapacitor performance [193,194].

Kaner et al is the first studied PANI as an electroactive material of supercapacitor [195] and Rudge studied the doping effect of PANI on its performance in supercapacitor [196]. Arbizzani et al reported that the

Table 4
Perovskite based electrode materials with electrochemical performances.

Electrode	Electrolyte	Characterization Method	E_{max} (Wh/kg)	P at E_{max} (W/kg)	Max Specific Capacitance (F/g)	Current density (A/g)	Scanning rate (mV/s)	Retention with cycle	*Reference*
$SrRuO_3$	6 M KOH	direct Optimizing pyrolysis			270		20		[175]
$Sr_{0.8}La_{0.2}Ru_{0.8}Mn_{0.2}O_3$	6 M KOH	pyrolysis route			160		20		[176]
$CaMnO_3$ Ca_2CuO_3 $Ca_3Co_2O_6$	5 M KOH	solid-state calcination and co-precipitation routes			384 275 997.9	1	5	96% @700	[168]
$La_{1-x}Al_xFeO_3$ & $LaFeO_3$	1 M H2SO4	chemical route			260		500		[178]
$La_{0.7}Sr_{0.3}NiO_{3-\delta}$	1 M Na_2SO_4	Electrospun	81.4	500	719	2			[183]
$La_xSr_{1-x}CoO_{3-\delta}$ ($0.3 \leq x \leq 1$)	1 M Na_2SO_4	Electrospun	34.8	400	747.75	2		97% @2000	[184]
$La_xSr_{1-x}Cu_{0.1}Mn_{0.9}O_{3-\delta}$ ($0.3 \leq x \leq 1$)	1 M Na_2SO_4	Electrospun	64.5	2k	464.5	2	50	@2000	[182]
$(La_{0.75}Sr_{0.25})_{0.95}MnO_{3-\delta}$ (LSM)/MnO_2	1 M Na_2SO_4	facile hydrothermal			437.2		2		[189]
$La_{0.85}Sr_{0.15}MnO_3$ & $LaMnO_3$	1 M KOH	Sol-gel			198 187	0.5			[190]
$La_xSr_{1-x}Co_{0.1}Mn_{0.9}O_{3-\delta}$ ($0.3 \leqslant x \ll 1$)	1 M KOH	electrospinning			485	1	5		[173]
$SrCo_{0.9}Nb_{0.1}O_{3-\delta}$ (SCN)	aqueous KOH	solid-state reaction	37.6	433.9	773.6 (gravimetric)	0.5	5	98.7% @ 3000	[188]

charge/discharge profile could be a line rather than flat plateau of battery like performance in a comparative study of various conducting polymers [197]. Bian and Yu developed de-doped PANI in which the specific capacitance is 29% higher than doped PANI [198]. Sharma and his coworker synthesized a nanoporous PANI with a specific area of 1059 $m^2 g^{-1}$ delivered a Sc of 410 Fg^{-1} [199]. Zhang et al reported that PANI nanofibers can deliver a Sc of 1210 Fg^{-1} [200] and depositing a thin layer of PANI onto porous carbon showed a high Sc of 2200 Fg^{-1} [201]. PANI/SWCNT supercapacitor delivered a Sc of 485 Fg^{-1} with a good cyclability [202]. A flexible sheet made of PANI-coated graphene nanofiber displayed a Sc of 976 Fg^{-1} at 0.4 Ag^{-1} [203]. Using PANI vertically on a graphene sheet with ordered alignment, a high Sc of 1665 Fg^{-1} has been achieved [204].

Hu and Chu employed iridium doped PANI film with an operating voltage window of 0.7-0.8 V [205]. Prasad and Miura electrodeposited MnO_x on PANI and achieved a Sc of 715 Fg^{-1} with only 3.5% in the specific capacitance loss after 5000 cycle [206]. Recently, a supercapacitor of $KCa_2Nb_3O_{10}$ perovskite/PANI has been reported to deliver a Sc of 250 Fg^{-1} [207] and a nano-composite of graphene/Fe_2O_3/PANI delivered a Sc of 638 Fg^{-1} with 92% capacity retention after 5000 cycles [208]. PANI growth on graphene/ZrO_2 exhibited a Sc of 1360 Fg^{-1} [209]. Polyprrolecand poly (3, 4-ethylenedioxythiophene) (PEDOT) delivered an excellent capability for supercapacitor as electrode [210,211]. Table 5 shows the electrochemical performance of various supercapacitors fabricating based on PANI electroactive material.

To get high capacitance, long lifetime, and great mechanical flexibility polymer binders were used to manufacture supercapacitor electrode materials. Nafion, polyvinylpyrrolidone (PVP), Poly-tetrafluoroethylene (PTFE), Poly-vinylidene difluoride, polyvinylidene chloride, Sulfonated poly-ether ether ketone (SPEEK) were some polymer binders and additives, which were used as integral component of supercapacitor electrode materials [220–222]. Conducting polymers have substantial differences with the inorganic materials utilized for supercapacitors because of the polymer matrix structure. While the lattice structure of most inorganic materials provides suitable places for the adsorption/intercalation of electroactive species within the material porosity at sub-surface, the polymer matrix has plenty of empty spaces, but the electroactive species does not simply fit in there and cause severe volume changes. The future of conducting polymer-based supercapacitor depends on the appropriate architecture of the corresponding nanocomposites.

3.2. Electrolyte

The electrolyte is another key component of ESs and provides ionic conductivity. The electrolyte within an electrochemical supercapacitor (ES) not only plays an influential role in EDLCs and reversible redox process for the charge storage but also determines the ES performance. The interaction between electrode and electrolyte material also plays an important role. Increasing the capacitance and cell voltage with a high specific area are the key to develop the ES. A large variety of electrolytes have been developed and reported in the literature to date. Aqueous electrolytes, organic electrolytes, ionic liquids electrolytes, redox-type electrolytes and solid or semi-solid electrolytes have been explored during the past several decades [77,223–225]. Liquid electrolytes can be further grouped into aqueous electrolytes, organic electrolytes and ionic liquids (ILs), while solid or quasi-solid state electrolytes can be broadly divided into organic electrolytes and inorganic electrolytes [226,227]. Fig. 13 shows the supercapacitor performance in the different electrolyte at 10 mV s^{-1} scan rate. There has been no perfect electrolyte developed, meeting all the requirements. Each electrolyte has its own advantages and disadvantages. In Tables 2–7, various electrolytes with different electrode materials have been reported. Table 6 shows different types of electrolyte-based supercapacitors and their performances.

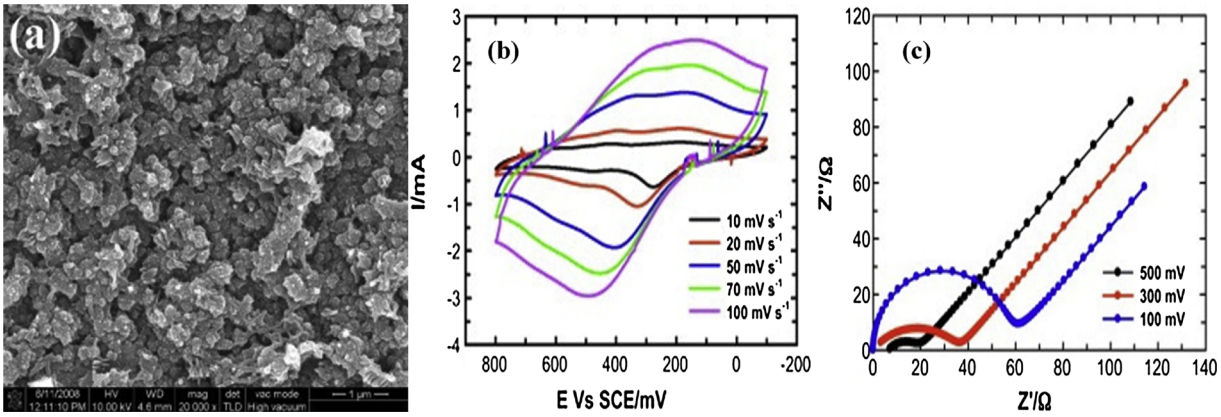

Fig. 12. (a) FESEM images, (b) CV curves at different scanning rates and (c) Nyquist plots at different potentials of polyaniline thin film [191].

Due to the narrow voltage windows, aqueous electrolytes are the low choice for commercial ES, though exhibit high conductivity. Aqueous electrolytes can be grouped into acid, alkaline and neutral solution in which H_2SO_4, KOH and Na_2SO_4 are the most frequently used electrolytes. There were more than a 10% loss in the specific capacitance of some asymmetric ESs after a certain number of cycle (1000–5000) using alkaline electrolytes for hybrid capacitors [229,230]. It is reported that a high energy density of 50 $Whkg^{-1}$ was achieved by using neutral electrolytes [231]. Due to the high operating potential window, organic electrolytes are suitable for ESs. Jiang et al. developed theoretical modeling and simulation of EDL using organic electrolytes, which may provide useful guidance EDLC design [232]. Among organic electrolytes, acetonitrile (ACN) and propylene carbonate (PC) is the most widely used solvents. 1 M LiTFSI/CAN used as organic electrolytes with carbon//V_2O_5 hybrid capacitor electrode exhibited wide operating cell voltage [233]. In the fuel cell vehicle application, ionic liquids (IL) are a good solution to improve the performance of ES [234]. Other than IL, some good key components as electrolyte materials have been identified, which can improve ES performance. Fig. 13: (a) Variation of supercapacitor performance of LiCl and LiOH electrolyte and (b) Variation of the capacitance with pressure in different electrolyte [190].

4. Hybrid supercapacitor

Instead of using graphene, metal oxides and polymers separately, combining each other we can get low cost, good electrical conductivity, mechanical flexibility and good chemical stability as hybrid electrode materials for supercapacitors.

Hybrid electrode configurations show considerable potential, consisting of two different electrodes made of different materials. Composite electrodes consist of one type of material incorporated into another within the same electrode. During research into polymer electrodes at the University of Bologna it was found that a sufficiently high polymer concentration could not be realized in the negative electrode. The positive polymer electrode was successfully constructed, however, and activated carbon was used as the negative electrode. This hybrid configuration resulted in a supercapacitor that outperformed a cell comprised of two carbon electrodes [38]. Also, of interest are the results of experiments into depositing polymers onto carbon substrates to form composite electrodes. Fig. 4 (d) & (e) presents various commercial hybrid supercapacitors.

In the past few years, research focus is directed toward the development of hybrid electrochemical capacitors (HECs), which asymmetrically and simultaneously store charges by surface ion adsorption/desorption on the cathode and by lithium/sodium-de/intercalation in the anode. HECs, including lithium-ion capacitors (LICs) and sodium-ion capacitors (NICs), are expected to bridge the gap between high-energy LIBs/sodium-ion batteries (SIBs) and high-power ECs, becoming the ultimate power source for electric vehicles and uninterruptible power systems [250–252]. One of the major issues for HECs, however, is the imbalance in the charge/discharge rate between the two electrodes due to the intrinsic differences in the energy-storage mechanisms. Under the normal operating conditions of a HEC, this imbalance in the kinetics prevents full energy utilization of the intercalation electrode and imposes a high overpotential in the capacitive electrode, thus deteriorating the overall efficiency. Using high-rate-intercalation pseudocapacitive materials as the anode is promising to balance the kinetics and power capability of both electrodes. The insertion-type materials are broadly classified into metal oxides, lithium/sodium metal oxide-based composites, transition metal carbides, and transition metal dichalcogenides and so on. Particularly, some kinds of electrode material, such as lithium and sodium metal-based materials and rutile TiO_2, cannot be defined as pseudocapacitive materials because of their voltage plateaus and phase changes during the de (intercalation) process. But their high rate capabilities ensure their applicability as high-rate electrodes in hybrid capacitors. Fig. 14 shows the various characteristics of a hybrid supercapacitor.

Dr. Yamabe from Kyoto University first discovered PAS (polyacenic semiconductive) material in 1981, collaboration with Dr. Yata from Kanebo Co. It is prepared by the pyrolysis of phenolic resin at 400–700 °C and amorphous carbonaceous material have excellent features as the electrode for high-energy-density rechargeable devices. The related patents were filed in the early 1980s by Kanebo Co and started to develop towards the commercialization of PAS battery and lithium ion capacitor (LIC). The PAS battery was put in use in 1986 and LIC in 1991 [253].

Hybrid supercapacitors attempt to exploit the relative advantages and mitigate the relative disadvantages of EDLCs and pseudocapacitors to realize better performance characteristics. Utilizing both Faradaic and non-Faradaic processes to store charge, hybrid capacitors have achieved energy and power densities greater than EDLCs without the sacrifices in cycling stability and affordability that have limited the success of pseudocapacitors. Research has focused on three different types of hybrid capacitors, distinguished by their electrode configuration [254]:

- Asymmetric hybrids
- Battery-type hybrids
- Composite hybrids

Asymmetric hybrids combine Faradaic and non-Faradaic processes by coupling an EDLC electrode with a pseudocapacitive electrode [17,254]. In principle, as a negative electrode usually carbon-based material is used, and as a positive some pseudocapacitive materials. The combination of a negative carbon electrode with a conducting polymer

Table 5
Conducting Polymer based electrode materials with electrochemical performances.

Electrode	Electrolyte	Characterization Method	E_{max} (Wh/kg)	P at E_{max} (W/kg)	Max Specific Capacitance (F/g)	Current density (A/g)	Scanning rate (mV/s)	Retention with cycle	Reference
PANI	1 M H_2SO_4	Chemical bath deposition	96.23	8.88 k	503		10	85% @1000	[191]
PANI-GNR-CNT	PVA/H_3PO_4	Situ polymerization			890	0.5	10	89% @1000	[212]
PANI	Gel polymer	Electrochemical deposition	188	1.4 k	672	17 m Acm^{-2}		@1000	[213]
PANI nanowires	1 M H_2SO_4	Electrochemica deposition	68	16 k	818	1		92% @1500	[214]
PANI nanowires arrays	1 M $HClO_4$	Facial one-step template-free	130	700	950	1	20	94% @400	[215]
Sulfonated PANI	1 M H_2SO_4	Aniline initiated polymerization	31.4	14.8 k	1107	1	10	94% @5000	[216]
Platinized tantalum foil substrate PANI	4 M HBF_4	Electrochemical deposition	2.7	1000	74	5 m Acm^{-2}	10	95% @20,000	[217]
PANI-CBf	0.5 M H_2SO_4	Wet chemical	412	40 k	1486	2	20	82% @500	[218]
PANI/SWCNT	1 M H_2SO_4	Chemical deposition	228	2250	485	5 m Acm^{-2}		95% @20,000	[191]
Oriented arrays PANI/expanded graphite Nano sheets	1 M H_2SO_4	Situ polymerization			1665	1	100	97% @2000	[204]
rGO-f/PANI	1 M H_2SO_4	Dipping and dry	17.6	98 k	790	1	10	80% @5000	[219]
PANI/MoS_2 nanocomposite	1 M H_2SO_4	Chemical deposition	265	18 k	575	1	20	98% @500	[191]
PANI-MnO_2	0.1 M Na_2SO_4	Electrochemical deposition	200		725	5 m Acm^{-2}	200	96.5% @5000	[206]

or metal oxide positive electrode received a great deal of attention [255,256]. Asymmetric hybrid capacitors that couple these two electrodes reduce the extent of this trade-off to achieve higher energy and power densities than comparable EDLCs. Also, they have better cycling stability than comparable symmetric pseudocapacitors [254,257,258].

Similarly, to asymmetric hybrids, the battery-type hybrids couple two different electrodes; however, the battery-type hybrids are unique in the combination of a supercapacitor electrode with a battery electrode. This configuration replicates the demand for higher energy supercapacitors and higher power batteries, combining the energy characteristics of batteries with the power, cycle life, and recharging times of supercapacitors [254]. Although there is less experimental data on battery type hybrids than on other types of supercapacitors, the data that is available suggests that these hybrids may be able to bridge the gap between supercapacitors and batteries. Despite the promising results, the consensus is that more research will be necessary to determine the full potential of battery-type hybrids [259].

Composite electrodes integrate carbon-based materials with either conducting polymer or metal oxide materials and incorporate both physical and chemical charge storage mechanisms together in a single electrode. The carbon-based materials facilitate a capacitive double-layer of charge and provide a high-surface-area backbone that increases the contact between the deposited pseudocapacitive materials and electrolyte. The pseudocapacitive materials can further increase the capacitance of the composite electrode through Faradaic reactions [254,260]. The synergetic mechanism could improve corrosion stability, increased the specific capacitance and the operating potential windows. Many different materials have been investigated, mostly exotic and very expensive (starting materials and preparation procedures) for asymmetric composite supercapacitors [261–263]. Fig. 15 presents the possible combinations of all hybrid supercapacitors.

Recently many scientists developed hybrid supercapacitors for different applications. Table 7 shows the electrical performance of various hybrid supercapacitors. Mastragostino et al. reported that a hybrid p-type poly (3-methylthiophene) (pMeT)/AC supercapacitor delivered higher average and maximum specific power and higher specific energy than n- and p-type pMeT supercapacitor in a double-layer activated carbon supercapacitor (DLCSs) [234]. He and his co-workers also developed a hybrid supercapacitor (AC/1-buthyl-3-methyl-imidazolium/pMeT), showed a Sc of 115 Fg^{-1} [223]. Gomez-Romero et al developed organic-inorganic hybrid nanocomposite materials for energy storage in solid-state electrochemical capacitors [264]. $Li_4Ti_5O_{12}$ nanostructured as anode and AC as cathode exhibited a specific energy 11 $Whkg^{-1}$ with the specific power of 800 Wkg^{-1} at 95% efficiency [265]. Zhang and Gong et al. made a self-stacked solvated graphene films (SSG) in flexible solid-state supercapacitor [118]. SSG films exhibited a high gravimetric Sc of 245 Fg^{-1}. Maher et al. developed hybrid supercapacitors and micro-supercapacitors for high-performance integrated energy storage with the energy density between 22 ~ 42 Whl^{-1} and power densities up to ~10 kWl^{-1}, which is 100 times faster than high-power lead-acid batteries and 1000 times faster than a lithium thin-film battery [266].

Songhun et al. reported a mesoporous niobium pentoxide/carbon as anode material which showed excellent energy density of 74 $Whkg^{-1}$ and power density of 18,510 Wkg^{-1} [267]. Lee et al. developed an asymmetric hybrid supercapacitor using AC as the cathode and urchin-like TiO_2 as the anode, which showed a Sc of 61.2 Fg^{-1} and energy density of 50.6 $Whkg^{-1}$ at a power density of 194.4 $kW\,kg^{-1}$ [268,269,268,269]. Xie et al. fabricated graphene-MnO_2 3D nanocomposite hybrid electrode using Ni foam produce 1.42 Fcm^{-2} areal capacitance at a mass loading of 9.8 $mg\,cm^{-2}$ [270]. Yongsheng et al. fabricated Fe_3O_4/graphene as the electrode for hybrid energy storage, which exhibited high reversible Sc of 1000 mAhg-1 at 90 mAg-1 [271]. Fe_3O_4/G//3D graphene showed energy density of 147 $Whkg^{-1}$ at a power density of 150 Wkg^{-1}. AC@La_2NiO_4/NiO exhibited a Sc of 710 Fg^{-1} at a scan rate of 1 mVs^{-1} in 7 M KOH electrolyte [272]. A Sc of

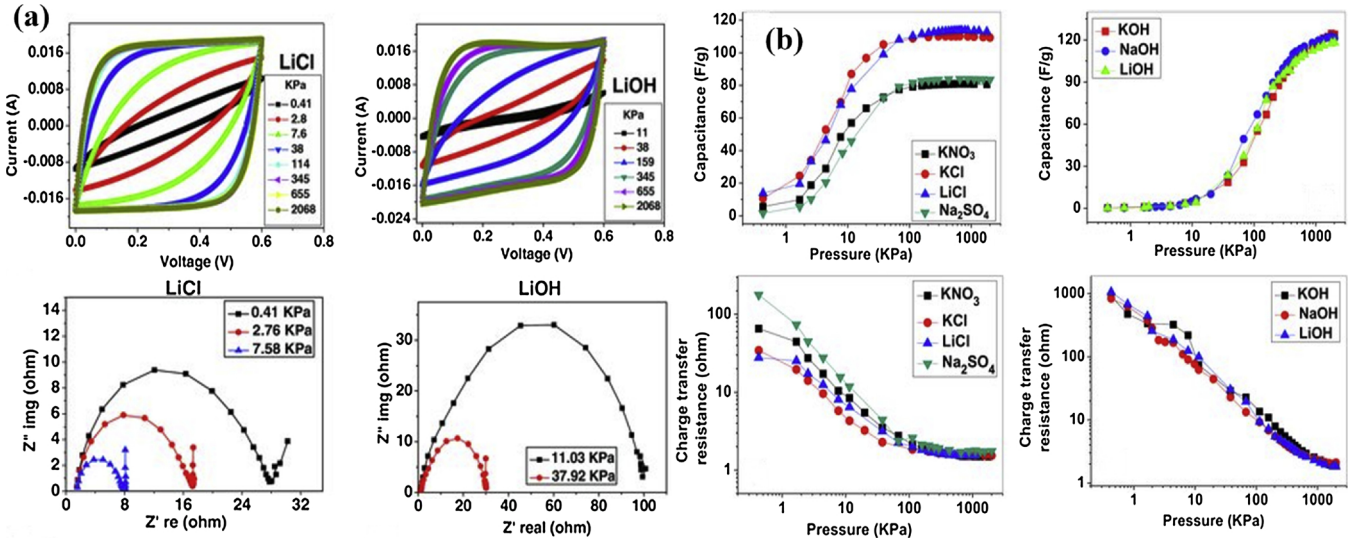

Fig. 13. (a) Variation of supercapacitor performance of LiCl and LiOH electrolyte and (b) Variation of the capacitance with pressure in different electrolyte [228].

1382 Fg^{-1} at 1 Ag^{-1} was obtained by hollow sphere NiS_2 as hybrid supercapacitor electrode material [273]. Zhou reported that *T*-Nb_2O_5/MNSs/rGO showed a power density of 25,600 Wkg^{-1} and a Sc of 86 Fg^{-1} [274]. Kwan et al. reported NiAl-LDH-NF as electrode material which showed a Sc of 1250 Cg^{-1} at 2 Ag^{-1} and LDH-NF as positive and GNS-NF as negative electrode delivered high energy density 30.2 $Whkg^{-1}$ at a power density of 800 Wkg^{-1} [70]. NMO/MWCNT/PEPOT exhibited a Sc of 836.27 Fg^{-1} [275]. Vlad et al. designed high energy and high power battery electrodes by hybridizing a nitroxide-polymer redox supercapacitor with a Li-ion battery material ($LiFePO_4$) [276].

PTMA = poly (2, 2, 6, 6-tetra-methyle-1-piperinidyoxy-4-4-methacrylate); PEDOTT = poly (3,4 ethylenedioxythiophene); EC = ethylene carbonate; DEC = diethyl carbonate; DMC = dimethyl carbonate; LDH-NF = layard double hydroxide-nickel foam; PTFE = polytetraflu oroethylene.

All other based electrode materials were not enough individually to get high performance in supercapacitor application. By making composite materials as hybridization can only possible to get high performance. The need for hybrid supercapacitors can be justified due to the limitations of current energy storage devices. Each type of supercapacitors like EDLC and pseudocapacitor find their applications as per their tendency. This factor limits their broader usage and as such, it is essential to develop hybrid supercapacitor systems to increase the applicability range. The applications of the hybrid supercapacitors are on the rise especially in the field of hybrid energy vehicles.

5. Perspectives

Supercapacitors have some advantages and disadvantages. Unlike batteries, because there is no chemical reaction going on, the charge-discharge cycle life of a supercapacitor is almost unlimited. Supercapacitors have higher specific power than most batteries, but low energy density. They provide peak power and backup power, energy storage and source balancing when used with energy harvesters. Supercapacitors minimize space requirement, size and weight, so it is cost effective storage and meets environmental standards. They have high self-discharge as compared to electrochemical batteries and do not support AC applications. They are used in applications with fluctuating loads such as laptop computers, GPS, photovoltaic systems and portable devices. With steady progress, supercapacitors are getting traction in these mainstream application markets such as the low-power equipment power buffer, voltage stabilizer, and temporary energy storage devices for energy harvesting system, incorporation into batteries, aviation and military instruments, the automotive and rail sectors and opening new possibilities in emerging sectors. The performance characteristics of supercapacitors are suiting them for applications requiring a high number of rapid charge and discharge cycles and for systems implementing energy recovery. These include hybrid-electric vehicles,

Table 6
Different electrolyte materials with electrochemical performances.

Electrolyte	Electrode	Specific Capacitance (F/g)	Cell voltage (V)	E_{max} (Wh/kg)	P at E_{max} (W/kg)	Reference
Aqueous electrolyte						
2 M H_2SO_4	MMPGC	105 at 4 mVs^{-1}	0.8	4	20	[235]
1 M H_2SO_4	ANS-rGO	375 at 1.3 Ag^{-1}	2	213	1328	[236]
1 M H_2SO_4	PANI-grafted rGO	1045.51 at 0.2 Ag^{-1}	0.8	8.3	60000	[237]
6 M KOH	p-CNn/CGBs	202 at 0.325 Ag^{-1}	0.9	4.9	150	[238]
2 M KOH	Poros $NiCo_2O_4$ nanotubes	1647.6 at 1 Ag^{-1}	0.41	38.5	205	[239]
1 M KCl	MnCl-doped PANI/SWCNTs	546 at 0.5 Ag^{-1}	1.6	194.13	~ 500	[240]
1 Li_2SO_4	Mesoporous MnO_2	284.24 at 1 mVs^{-1}	1	~ 28.8	~ 70	[241]
1 M Na_2SO_4	Hydrous RuO_2	52.66 at 0.625 Ag^{-1}	1.6	18.7	500	[242]
Organic electrolyte						
1 M $TEABF_4$/ACN	Highly poros interconnected carbon nanosheets	~ 120-150 at 1 mVs^{-1}	2.	25	25000-27000	[243]
1.6 M TEAODFB/PC	AC	21.4 at 1 Ag^{-1}	2.5	~ 28	~ 1000	[244]
1 M $LiPF_6$/(EC-DEC 1:1)	Heteroatom doped porous carbon flakes	126 at 1 Ag^{-1}	3	29	2243	[245]
0.5 M B_4NBF_4/ACN	Heterostrctred poly(3,6-dithien-2-yl-9H-carbazol-9-yl acetic acid)/TiO_2 nanoparticles composite	462.88 at 2.5 Ac^{-2}	1.2	89.98		[246]
1 M LiTFSI/ACN	MnO_2 nanorodes-rGO//V_2O_5 NWs-rGO	36.9	2	15.4	436.5	[247]

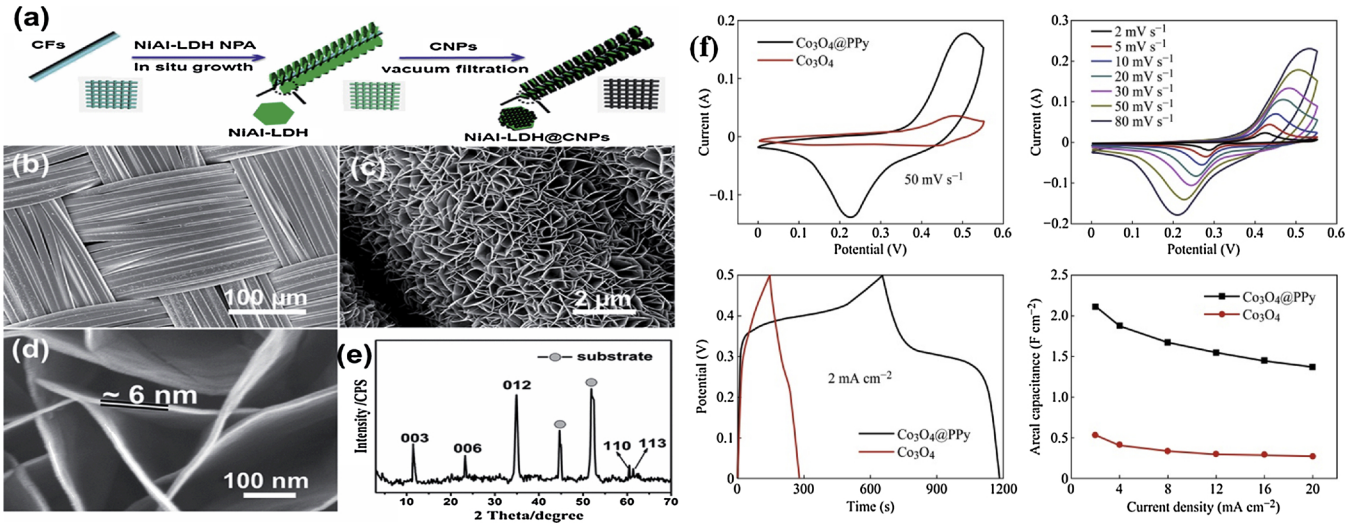

Fig. 14. (a) Schematic illustration showing the fabrication of the LDH@CNPs hybrid electrode; (b) SEM image of the conductive fibers (CFs); (c) and (d) top-view SEM images of the NiAl-LDH NPAs on the surface of CFs; (e) XRD pattern of as-prepared LDH NPAs on CF [248] and (f) cyclic voltammetry and charge-discharge with areal capacitances of the Co_3O_4@ppy hybrid electrode at a scan rate of 50 mV s^{-1} with a current density of 2 mA cm^{-2} [249].

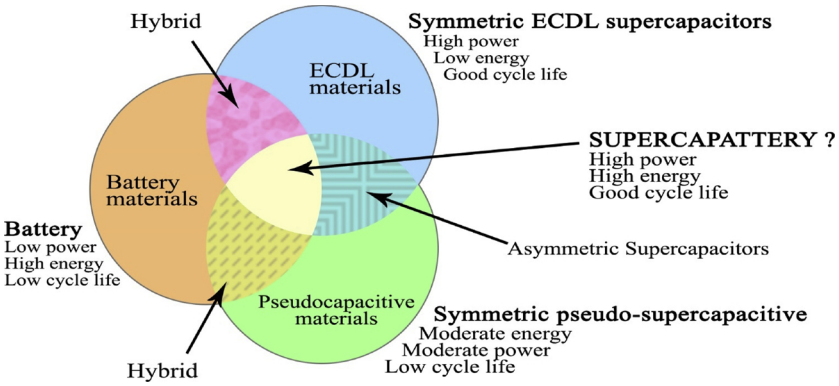

Fig. 15. Merging the characteristics of hybrid supercapacitors.

wind turbines, rail transit, consumer electronics, and electric grid systems.

Supercapacitors continue to gain usage as more applications require storing and releasing high amounts of energy in short periods. Market research studies continue to project a bright future for the technology. As of 2016 worldwide sales of supercapacitors is about US$400 million [289]. One recent study, by Zion Market Research of Sarasota, Florida, projects the supercapacitor market to grow from $684.7 million in 2016 to over $2 billion by 2022, at a compound annual growth rate of 20.5%. Another recent study, by Research and Markets, projects the supercapacitor market to grow at a compound annual growth rate of 18.6% from 2017 through 2022, reaching $2.44 billion [290]. IDTechEx estimates that the high-power energy storage market is expected to grow almost ten-fold to $2 billion a year by 2026 up from about $240 million currently, Supercapacitors could capture about $800 million to $1 billion of that potential market opportunity [291]. The study adds that the limitations to more rapid growth include high supercapacitor prices and the lack of industry-wide experience. Supercapacitor manufacturers continue to improve the power handling and performance of their parts. Table 8 shows differences among capacitors of various manufacturers in capacitance range, cell voltage, specific power and energy [21,79].

Scientists continue to look at new applications and materials for supercapacitors. Current applications include the automotive industry, hybrid transportation systems around the world, grid stabilization, utility vehicles, and rail-system power models. One of the coolest applications that's already available is the combination of supercapacitors with fuel cells for maximized energy storage and rapid charging capabilities. Recently, researchers at UCLA and the University of Connecticut developed a bio-friendly energy storage system called a biological supercapacitor, which operates using charged particles, or ions, from fluids in the human body. The research team envisions the supercapacitor leading to longer-lasting cardiac pacemakers and other implantable medical devices. Scientists are researching to develop new and advanced materials (hybrid) for better performance in supercapacitor applications and looking at alternative materials to the conventional carbon, which requires high processing temperatures and the use of harsh chemicals to produce [292–296]. Scientists are also looking at alternative materials to conventional carbon, which require high processing temperatures and the use of harsh chemicals to produce. Researchers at the Massachusetts Institute of Technology developed a supercapacitor that uses no conductive carbon, instead of employing a series of metal organic frameworks that provide a large surface area. To develop and boost the performances, scientists and researchers have explored and modified materials structures modified from certain ways to deliver high power and energy as covalent organic frameworks (COFs), metal-organic frameworks (MOFs), MXenes, metal sulphides, metal nitrides, mixed conductors, ultrafast 2D, 3D materials and 2D to 3D structures [297]. Recent developments and innovations in the materials used in supercapacitors manufacturing mainly center on reducing the possibility of self-discharge or short circuit. Stakeholders in the supercapacitor market are aiming to capitalize on various

Table 7
Hybrid electrode materials with electrochemical performances.

Electrode	Electrolyte	Characterization Method	E_{max} (Wh/kg)	P at E_{max} (W/kg)	Max Specific Capacitance (F/g)	Current density (A/g)	Scanning rate (mV/s)	Retention with cycle	Reference
T-Nb_2O_5 MNSs/rGO//MC/rGO	1 M $LiPF_6$ in EC and DMC	Solvo-Hydrothermal and annealing	56 21	88 25,600	181 $mAhg^{-1}$	20m	10	82% @4000	[274]
Li4Ti_5O_{12} (anode)/activated carbon (cathode)	NaOH	Wet chemical	11	800				95% @10,000	[265]
TiO_2 with activated carbon	10 M NaOH	Hydrothermal	50.648	194.412	61.1	3		93% @10,000	[269]
Activated carbon/$LaNiO_4$/NiO	7 M KOH	Wet chemical	70.37	32.4 k	710 48	1	1		[272]
NiO with 3D nano composite graphene		Chemical vapor deposition			816		5	@2000	[277]
$Sn_{0.95}Al_{0.05}H_{0.05}P_2O_7$-PTFE	H_3PO_4	Wet chemical	32	12	210	3	10	83% @7000	[278]
Co_3O_4 nanowire with 3D graphene foam		Chemical vapor deposition			1100	10		@500	[279]
$LiFePO_4$-PTMA		Situ polymerization			170 $mAhg^{-1}$	0.8	1	88% @1500	[276]
rGN/PANI		Dilute polymerization	65.94	0.2k	740	0.5		87% @1000	[280]
PANI/GO Nano sheets	1 M H_2SO_4	Nanoscale blending			375	0.5	10	90.7% @500	[281]
rGO/PANI/eCFC	1 M H_2SO_4	Situ polymerization	25.4	92.2 k	1145	1	10	94% @5000	[282]
MnO_2 with thermally rGO	3 M KCl	Thermal reduction	50.2	365			5m	~ 100% @1500	[283]
NMO/MWCNTs/PEDOTT	6 M KOH	Chemical oxidation polymerization			836.27	10	5		[284]
RuO_2 with GO	1 M H_2SO_4	Sol-gel and annealing	20.1	50	570	0.1	1	97.9% @1000	[285]
Co_3O_4 with hydrothermally rGO	2 KOH	Hydrothermal	39	8.3k	472		2	95.6% @1000	[286]
NiO flakes with GO	1 M KOH	Electrophoretic and chemical-bath deposition	16.8		400	2		94% @2000	[287]
Fe_3O_4/graphene nanocomposite//3D graphene	EC/DEC/DMC	Solvothermal	147	150	1000 $mAhg^{-1}$ 704 $mAhg^{-1}$	90 m 2700 m		70% @1000	[271]
Activated carbon//Poly(3-methylthiophene)	1 M 1-buthyl-3-methyl-imidazolium	Polymerization	32	17 k	115		20		[223]
LDH-NF & LDH-NF-H	6 M KOH	LPD	30.2		1250 C g^{-1}	50		76.7% @5000	[70]
3D Laser-scribed graphene/MnO_2	1 M Na_2SO_4	Electrochemical deposition	42 W h/l	10 k W/l	1197 F/cm3		1000	96% @10,000	[266]
NiS hollow sphere	2 M KOH	Hydrothermal			1382 451.1	1 10	5-60	@5000	[273]
Mesoporous m-Nb_2O_5/carbon/MSP-20		One-pot	74	18,510	115.1 $mAhg^{-1}$	5000 m	2-50	90% @1000	[267]
Activated carbon/urchin-like TiO_2	1.5 M $LiPF_6$ in EC-DMC	Hydrothermal	50.6	194.4	61.2	3	10	89% @5000	[268]
V_2O_5 nanorods with solvothermally rGO	8 M LiCl	Solvothermal and annealing	74.58	500	537	1		84% @1000	[288]

Table 8
Electrical performances of supercapacitors of different manufacturers.

Manufacturer	*Series name*	*Capacitance range (F)*	*Cell voltage (V)*	*Specific power (95%) (W/kg)*	*Specific energy (Wh/kg)*	*Remarks*
APowerCap	APowerCap	4–2800	2.7	900	≤ 4.5	–
AVX	BestCap	0.05–0.56	3.6	–	≤ 0.13	Modules up to 20 V
Asahi Glass	–	1375	2.7	390	4.9	–
BatScap	–	1680	2.7	2050	4.2	–
Cap-XX	Cap-XX	0.17–2.4	2.5	≤ 2.2	–	–
CDE	Ultracapacitor	0.1–1.0	3.6	–	–	–
Cooper	PowerStor	0.22–3000	2.5/2.7	¬	–	Modules up to 62 V
Elna	DYNACAP POWERCAP	0.047–1500	2.5/3.6	–	–	–
Evans	Capattery	0.001–10	5.5…125	–	–	Hybrid capacitors
FastCAP Systems	EEx	340–460	1-3	≤ 10.5	–	–
Green Tech	Supercapacitor	2–600	2.7/2.8	–	–	Modules up to 64 V
Illinois	Supercapacitor	0.3800	2.3/2.7	≤ 8.6	≤ 6.6	–
Ioxus	Ultracapacitor	100–3000	2.7	≤ 8.7	≤ 6.4	Modules up to 130 V
JSR Micro	Ultimo	1100–3300	3.8	≤ 20	≤ 12	Li-Ion-capacitors
Korchip	STARCAP	0.02–400	2.5/2.7	≤ 7.0	≤ 6.1	–
LS Mtron	Ultracapacitor	100–3400	2.7/2.8	900	4.45	Modules up to 130 V
Maxwell	Boostcap	1–3400	2.2/2.8	–	≤ 6.0	Modules up to 160 V
Murata	EDLC	0.22–1.0	4.2/5.5	≤ 2.7	≤ 3.1	2 cells in series
NEC Tokin	Supercapacitor	0.047–200	2.7/11	–	–	–
Nesscap	EDLC. Pseudocapacitor	3–1800 50–5085	2.7	975 958	≤ 4.5 ≤ 8.7	Modules up to 125 V
Nichicon	EVerCAP	1.0–6000	2.5/2.7	–	–	–
NCC, ECC	DLCCAP	350–2300	2.5	–	–	–
Panasonic	Goldcap	0.1–1200	2.3/2.5	514	2.3	Modules up to 15 V
Power Sys (PC)	–	1350	2.7	650	4.9	–
Samwha	Green-Cap ESD-SCAP	3–7500	2.5/2.7	≤ 7.6	≤ 7.0	–
Skeleton	SkelCap	250–4500	2.85	≤ 14.1	≤ 10.1	Modules up to 350 V
Taiyo Yuden	PAS Capacitor LIC Capacitor	0.5–20 0.5–270	2.5/3.0 3.8	– –	– –	Pseudocapacitors Li-Ion-capacitors
VinaTech	Hy-Cap	1–500	2.3/3.0	≤ 8.7	≤ 6.3	–
Vishay	ENYCAP	4–15	1.4	–	–	Modules up to 8.4 V
WIMA	SuperCap	100–3000	2.5	–	–	Modules up to 28 V
YEC	Kapton capacitor	0.5–400	2.7	–	–	–
Yunasko	Ultracapacitor	480–1700	2.7	–	–	Modules up to 48 V

performance characteristics of pseudo-capacitors and hybrid capacitors, which can reflect higher energy density than any other types of supercapacitors. In the coming years, supercapacitors are likely to witness ubiquitous acceptance in various industry verticals. The future of supercapacitors market is likely to witness the emergence of ECs that will power the future of modern wearables and consumer electronic products. Solar supercapacitors are also a thing from future, which is expected to have a huge sales potential in the wearable sensors landscape, especially in wearable health devices. The ongoing research activities and developments in the power electronics industry continue to hint at supercapacitors replacing batteries soon. The exponential growth rate of the supercapacitors market is expected to amplify lucrative opportunities for researchers, manufacturers, and other stakeholders in the landscape.

6. Conclusion

Supercapacitors were relegated to mundane applications such as memory protection and internal battery backup, but in the last few years, the application space has broadened significantly into hybrid vehicles, smartphones, and energy harvesting. New technologies on the horizon promise to bring supercapacitors into full competition with rechargeable batteries.

In this review, we gathered different electrode and electrolyte materials with their performances, pointing out their advantages and disadvantages in supercapacitors. To realize the expected full-scale practical application, the quality and reproducible quantity of the electrode and electrolyte materials both will have to be further improved, with the development of the most desired structures tunable in nano-, micro-, meso- and macroscales. The selected methods should be able to produce materials with a controllable particle size that can cater for supercapacitor applications. Therefore, nano-dimensional materials have received tremendous acceptance due to their capability to enhance the capacitive performance of the supercapacitor systems while maintaining high cycle life and great kinetic reversibility. On the other hand, the potential of carbonaceous materials like activated carbon, carbon-nanotubes, graphite and graphene in supercapacitor application should be taken note of. Nowadays, a combination of carbons with metal oxides, perovskites or conducting polymers to form composite or hybrid supercapacitors may portray as another interesting alternative or remarkable breakthrough in these energy-related applications. Batteries and supercapacitors combined to offer the best solution for many energy systems from the automotive sector to grid energy storage, allowing batteries not only to perform better but also to extend their life whilst reducing both CAPEX and OPEX. The supercapacitor industry is carving its place in the future of energy systems. Manufacturers based in the USA, Asia and recently Europe are set to address market needs in the automotive sector, aerospace, public transport and rail, and the future smart grids and many more. Finally, we suggest that supercapacitors become an emerging energy storage technology that will take a key role in the future of energy systems.

Acknowledgement

One of the authors, Ahmed Afif, gratefully acknowledge the University Graduate Scholarship of Universiti Brunei Darussalam. This work was made under the project no. UBD/RSCH/URC/RG(b)/2018/002.

References

[1] S. Ould Amrouche, D. Rekioua, T. Rekioua, S. Bacha, Overview of energy storage in renewable energy systems, Int. J. Hydrogen Energy 41 (45) (2016) 20914–20927.
[2] L. Jiang, L. Wang, R. Wang, F. Zhu, Y. Lu, A.P. Roskilly, Experimental

investigation on an innovative resorption system for energy storage and upgrade, Energy Convers. Manag. 138 (2017) 651–658.
[3] S.P.S. Badwal, S.S. Giddey, C. Munnings, A.I. Bhatt, A.F. Hollenkamp, Emerging electrochemical energy conversion and storage technologies, Front. Chem. 2 (September) (2014) 79.
[4] F. Bonaccorso, et al., 2D materials. Graphene, related two-dimensional crystals, and hybrid systems for energy conversion and storage, Science (80-.) 347 (6217) (2015) 1246501.
[5] M.G. Junior, et al., Functional nanomaterials for applications in energy storage and conversion, Recent Advances in Complex Functional Materials (2017) 217–237 Springer.
[6] A. Afif, N. Radenahmad, Q. Cheok, S. Shams, J.H. Kim, A.K. Azad, Ammonia-fed fuel cells: a comprehensive review, Renew. Sustain. Energy Rev. 60 (2016) 822–835.
[7] N. Radenahmad, A. Afif, P.I. Petra, S.M.H. Rahman, S.-G. Eriksson, A.K. Azad, Proton-conducting electrolytes for direct methanol and direct urea fuel cells – a state-of-the-art review, Renew. Sustain. Energy Rev. 57 (2016) 1347–1358.
[8] S. Hossain, A.M. Abdalla, S.N.B. Jamain, J.H. Zaini, A.K. Azad, A review on proton conducting electrolytes for clean energy and intermediate temperature-solid oxide fuel cells, Renew. Sustain. Energy Rev. 79 (2017) 750–764.
[9] A. González, E. Goikolea, J.A. Barrena, R. Mysyk, Review on supercapacitors: technologies and materials, Renew. Sustain. Energy Rev. 58 (2016) 1189–1206.
[10] K. Sharma, A. Arora, S.K. Tripathi, Review of supercapacitors: materials and devices, J. Energy Storage 21 (2019) 801–825.
[11] W.H. Low, P.S. Khiew, S.S. Lim, C.W. Siong, E.R. Ezeigwe, Recent development of mixed transition metal oxide and graphene/mixed transition metal oxide based hybrid nanostructures for advanced supercapacitors, J. Alloys Compd. 775 (2018) 1324–1356.
[12] W. Raza, et al., Recent advancements in supercapacitor technology, Nano Energy 52 (2018) 441–473.
[13] A. Muzaffar, M.B. Ahamed, K. Deshmukh, J. Thirumalai, A review on recent advances in hybrid supercapacitors: design, fabrication and applications, Renew. Sustain. Energy Rev. 101 (2019) 123–145.
[14] A. Burke, R&D considerations for the performance and application of electrochemical capacitors, Electrochim. Acta 53 (3) (2007) 1083–1091.
[15] N.A. Kyeremateng, T. Brousse, D. Pech, Microsupercapacitors as miniaturized energy-storage components for on-chip electronics, Nat. Nanotechnol. 12 (1) (2017) 7–15.
[16] B. Andrew, Ultracapacitors: why, how, and where is the technology, J. Power Sources 91 (1) (2000) 37–50.
[17] R. Kötz, M. Carlen, Principles and applications of electrochemical capacitors, Electrochim. Acta 45 (15–16) (2000) 2483–2498.
[18] A.S. Aricò, P. Bruce, B. Scrosati, J.M. Tarascon, W. van Schalkwijk, Nanostructured materials for advanced energy conversion and storage devices, Nat. Mater. 4 (5) (2005) 366–377.
[19] A. Chu, P. Braatz, Comparison of commercial supercapacitors and high-power lithium-ion batteries for power-assist applications in hybrid electric vehicles: I. Initial characterization, J. Power Sources 112 (1) (2002) 236–246.
[20] Jeff Kerns, What's the difference between batteries and capacitors, Machine Design, 2015 [Online]. Available: https://www.machinedesign.com/batteriespower-supplies/what-s-difference-between-batteries-and-capacitors . [Accessed: 22-Feb-2019].
[21] Supercapacitor, Wikiwand. [Online]. Available: http://www.wikiwand.com/en/Supercapacitor#/Styles. [Accessed: 17-Jul-2017].
[22] B.E. Conway, Electrochemical Supercapacitors: Scientific Fundamentals and Technological Applications, Springer Science & Business Media, 2013.
[23] J.M. Tarascon, M. Armand, Issues and challenges facing rechargeable lithium batteries, Nature 414 (6861) (2001) 359–367.
[24] M. Armand, J.-M. Tarascon, Building better batteries, Nature 451 (February 7179) (2008) 652–657.
[25] J.B. Goodenough, H.D. Abruna, M.V. Buchanan, Basic research needs for electrical energy storage, Report Basic Energy Sci. Workshop Elect. Energy Storage (2007).
[26] A.G. Pandolfo, A.F. Hollenkamp, Carbon properties and their role in supercapacitors, J. Power Sources 157 (1) (2006) 11–27.
[27] J. Wang, et al., Pseudocapacitive materials for electrochemical capacitors: from rational synthesis to capacitance optimization, Natl. Sci. Rev. 4 (1) (2017) 71–90.
[28] George Zheng Chen, How Do Compare the Specific Capacitance of Our System With Commercially Available Supercapacitor, ResearchGate GmbH, 2016 [Online]. Available: https://www.researchgate.net/post/How_do_compare_the_specific_capacitance_of_our_system_with_commercially_available_supercapacitor . [Accessed: 24-Feb-2019].
[29] B. Song, et al., Molecular level study of graphene networks functionalized with phenylenediamine monomers for supercapacitor electrodes, Chem. Mater. 28 (24) (2016) 9110–9121.
[30] B. Song, et al., Systematic study on structural and electronic properties of diamine/triamine functionalized graphene networks for supercapacitor application, Nano Energy 31 (2017) 183–193.
[31] D.P. Dubal, N.R. Chodankar, D.H. Kim, P. Gomez-Romero, Towards flexible solid-state supercapacitors for smart and wearable electronics, Chem. Soc. Rev. 47 (6) (2018) 2065–2129.
[32] X. Peng, L. Peng, C. Wu, Y. Xie, Two dimensional nanomaterials for flexible supercapacitors, Chem. Soc. Rev. 43 (10) (2014) 3303–3323.
[33] Y. Lin, Y. Gao, Z. Fan, Printable fabrication of nanocoral-structured electrodes for High-performance flexible and planar supercapacitor with artistic design, Adv. Mater. 29 (43) (2017) 1701736 (1–8).
[34] K. K, X. Chu, Electrochemical capacitors, The Electrochemical Society Proceedings Series, (1995), p. 171.
[35] B. McEnaney, T.J. Mays, H. Marsh (Ed.), Introduction to Carbon Science, Vol. 154 1989, p. 156.
[36] J.F.M.H. Byrne, Porosity in Carbons, (1995), pp. 12–14.
[37] S. Yoon, J. Lee, T. Hyeon, S.M. Oh, Electric double-layer capacitor performance of a New mesoporous carbon, J. Electrochem. Soc. 147 (7) (2000) 2507–2512.
[38] A. Namisnyk, J. Zhu, A survey of electrochemical super-capacitor technology, Australian Universities Power Engineering Conference, (2003).
[39] M.J. Sparnaay, The Electric Double Layer Vol. 4 Pergamon Press (Aust.) Pty. Ltd., Sydney, 1972.
[40] P. Simon, Y. Gogotsi, Materials for electrochemical capacitors, Nat. Mater. 7 (November 11) (2008) 845–854.
[41] Y. Gogotsi (Ed.), Carbon Nanomaterials, CRC Press, 2006.
[42] D.N. Futaba, et al., Shape-engineerable and highly densely packed single-walled carbon nanotubes and their application as super-capacitor electrodes, Nat. Mater. 5 (December 12) (2006) 987–994.
[43] C. Portet, J. Chmiola, Y. Gogotsi, S. Park, K. Lian, Electrochemical characterizations of carbon nanomaterials by the cavity microelectrode technique, Electrochim. Acta 53 (26) (2008) 7675–7680.
[44] C.M. Yang, et al., Nanowindow-regulated specific capacitance of supercapacitor electrodes of single-wall carbon nanohorns, J. Am. Chem. Soc. 129 (1) (2007) 20–21.
[45] H. Liu, L.-H. Jin, P. He, C. Wang, Y. Xia, Direct synthesis of mesoporous carbon nanowires in nanotubes using MnO2 nanotubes as a template and their application in supercapacitors, Chem. Commun. (44) (2009) 6813–6815.
[46] C. Largeot, P.L. Taberna, Y. Gogotsi, P. Simon, Microporous carbon-based electrical double layer capacitor operating at High temperature in ionic liquid electrolyte, Electrochem. Solid-State Lett. 14 (12) (2011) A174.
[47] C. Niu, E.K. Sichel, R. Hoch, D. Moy, H. Tennent, High power electrochemical capacitors based on carbon nanotube electrodes, Appl. Phys. Lett. 70 (11) (1997) 1480–1482.
[48] P. Azaïs, et al., Causes of supercapacitors ageing in organic electrolyte, J. Power Sources 171 (2) (2007) 1046–1053.
[49] T. Kinjo, T. Senjyu, N. Urasaki, H. Fujita, Output levelling of renewable energy by electric double-layer capacitor applied for energy storage system, IEEE Trans. Energy Convers. 21 (1) (2006) 221–227.
[50] J. Garthwaite, How ultracapacitors work (and why they fall short), Earth2Tech. GigaOM Netw. (2011) 6–13.
[51] B.E. Conway, V. Birss, J. Wojtowicz, The role and utilization of pseudocapacitance for energy storage by supercapacitors, J. Power Sources 66 (1–2) (1997) 1–14.
[52] B.E. Conway, Transition from 'supercapacitor' to 'battery' behavior in electrochemical energy storage, J. Electrochem. Soc. 138 (6) (1991) 1539–1548.
[53] V. Augustyn, P. Simon, B. Dunn, Pseudocapacitive oxide materials for high-rate electrochemical energy storage, Energy Environ. Sci. 7 (5) (2014) 1597–1614.
[54] Z. Wu, Y. Zhu, X. Ji, NiCo 2 O 4-based materials for electrochemical supercapacitors, J. Mater. Chem. A 2 (36) (2014) 14759–14772.
[55] A.M. Bryan, L.M. Santino, Y. Lu, S. Acharya, J.M. D'Arcy, Conducting polymers for pseudocapacitive energy storage, Chem. Mater. 28 (17) (2016) 5989–5998.
[56] Y.M. Volfkovich, A.A. Mikhailin, D.A. Bograchev, V.E. Sosenkin, V.S. Bagotsky, Studies of supercapacitor carbon electrodes with high pseudocapacitance, Recent Trend Electrochemical Sci. Technol., InTech (2012) 159–182.
[57] E. Herrero, L.J. Buller, H.D. Abruña, Underpotential deposition at single crystal surfaces of Au, Pt, Ag and other materials, Chem. Rev. 101 (7) (2001) 1897–1930.
[58] S. Trasatti, G. Buzzanca, Ruthenium dioxide: a new interesting electrode material. Solid state structure and electrochemical behaviour, J. Electroanal. Chem. Interfacial Electrochem. 29 (2) (1971) A1–A5.
[59] A. Venkataraman, Pseudocapacitors for Energy Storage, Portland State University, 2015, pp. 1–81.
[60] K. Makgopa, et al., A high-rate aqueous symmetric pseudocapacitor based on highly graphitized onion-like carbon/birnessite-type manganese oxide nanohybrids, J. Mater. Chem. A 3 (7) (2015) 3480–3490.
[61] W. Chen, H. Yu, S.Y. Lee, T. Wei, J. Li, Z. Fan, Nanocellulose: a promising nanomaterial for advanced electrochemical energy storage, Chem. Soc. Rev. 47 (8) (2018) 2837–2872.
[62] E.E. Miller, Y. Hua, F.H. Tezel, Materials for energy storage: review of electrode materials and methods of increasing capacitance for supercapacitors, J. Energy Storage 20 (2018) 30–40.
[63] K. Shi, I. Zhitomirsky, Electrophoretic nanotechnology of graphene-carbon nanotube and graphene-polypyrrole nanofiber composites for electrochemical supercapacitors, J. Colloid Interface Sci. 407 (2013) 474–481.
[64] K. Shi, X. Yang, E.D. Cranston, I. Zhitomirsky, Efficient lightweight supercapacitor with compression stability, Adv. Funct. Mater. 26 (35) (2016) 6437–6445.
[65] Y. Liu, K. Shi, I. Zhitomirsky, New colloidal route for electrostatic assembly of oxide nanoparticle - carbon nanotube composites, Colloids Surfaces A Physicochem. Eng. Asp. 446 (2014) 15–22.
[66] Y. Liu, M.S. Ata, K. Shi, G.Z. Zhu, G.A. Botton, I. Zhitomirsky, Surface modification and cathodic electrophoretic deposition of ceramic materials and composites using celestine blue dye, RSC Adv. 4 (56) (2014) 29652–29659.
[67] K. Shi, I. Zhitomirsky, Fabrication of polypyrrole-coated carbon nanotubes using oxidant-surfactant nanocrystals for supercapacitor electrodes with high mass loading and enhanced performance, ACS Appl. Mater. Interfaces 5 (24) (2013) 13161–13170.
[68] K. Shi, K.P. Giapis, Scalable fabrication of supercapacitors by nozzle-free electrospinning, ACS Appl. Energy Mater. 1 (2) (2018) 296–300.
[69] D. Doennig, R. Pentcheva, Control of orbital reconstruction in (LaAlO3)M/(SrTiO3)N(001) quantum wells by strain and confinement, Sci. Rep. 5 (2015) 1–7.

[70] L. Zhang, K.N. Hui, K. San Hui, H. Lee, High-performance hybrid supercapacitor with 3D hierarchical porous flower-like layered double hydroxide grown on nickel foam as binder-free electrode, J. Power Sources 318 (2016) 76–85.
[71] C.D. Lokhande, D.P. Dubal, O.S. Joo, Metal oxide thin film based supercapacitors, Curr. Appl. Phys. 11 (3) (2011) 255–270.
[72] J.S. Lee, S.I. Kim, J.C. Yoon, J.H. Jang, Chemical vapor deposition of mesoporous graphene nanoballs for supercapacitor, ACS Nano 7 (7) (2013) 6047–6055.
[73] L.L. Zhang, X.S. Zhao, Carbon-based materials as supercapacitor electrodes, Chem. Soc. Rev. 38 (9) (2009) 2520–2531.
[74] S.W. Lee, B.M. Gallant, H.R. Byon, P.T. Hammond, Y. Shao-Horn, Nanostructured carbon-based electrodes: bridging the gap between thin-film lithium-ion batteries and electrochemical capacitors, Energy Environ. Sci. 4 (6) (2011) 1972–1985.
[75] Y. Zhai, Y. Dou, D. Zhao, P.F. Fulvio, R.T. Mayes, S. Dai, Carbon materials for chemical capacitive energy storage, Adv. Mater. 23 (42) (2011) 4828–4850.
[76] G. Wang, L. Zhang, J. Zhang, A review of electrode materials for electrochemical supercapacitors, Chem. Soc. Rev. 41 (2) (2012) 797–828.
[77] F. Béguin, V. Presser, A. Balducci, E. Frackowiak, Carbons and electrolytes for advanced supercapacitors, Adv. Mater. 26 (14) (2014) 2219–2251.
[78] Z. Yang, J. Tian, Z. Yin, C. Cui, W. Qian, F. Wei, Carbon nanotube- and graphene-based nanomaterials and applications in high-voltage supercapacitor: a review, Carbon N. Y. 141 (2019) 467–480.
[79] P. Simon, A. Burke, Nanostructured carbons: double-layer capacitance and more," electrochem, Soc. Interface 17 (1) (2008) 38–43.
[80] A.B. Fuertes, G. Lota, T.A. Centeno, E. Frackowiak, Templated mesoporous carbons for supercapacitor application, Electrochim. Acta 50 (14) (2005) 2799–2805.
[81] J. Gamby, P.L. Taberna, P. Simon, J.F. Fauvarque, M. Chesneau, Studies and characterisations of various activated carbons used for carbon/carbon supercapacitors, J. Power Sources 101 (1) (2001) 109–116.
[82] H. Shi, Activated carbons and double layer capacitance, Electrochim. Acta 41 (10) (1996) 1633–1639.
[83] D. Qu, H. Shi, Studies of activated carbons used in double-layer capacitors, J. Power Sources 74 (1) (1998) 99–107.
[84] D. Qu, Studies of the activated carbons used in double-layer supercapacitors, J. Power Sources 109 (2) (2002) 403–411.
[85] Y.J. Kim, et al., Correlation between the pore and solvated ion size on capacitance uptake of PVDC-based carbons, Carbon N. Y. 42 (8) (2004) 1491–1500.
[86] K. Izutsu, Electrochemistry in Nonaqueous Solutions, John Wiley & Sons, 2009.
[87] Y. Marcus, Ion Solvation, Wiley, 1985.
[88] K. Jurewicz, et al., Capacitance properties of ordered porous carbon materials prepared by a templating procedure, J. Phys. Chem. Solids 65 (2) (2004) 287–293.
[89] J.A. Fernández, T. Morishita, M. Toyoda, M. Inagaki, F. Stoeckli, T.A. Centeno, Performance of mesoporous carbons derived from poly (vinyl alcohol) in electrochemical capacitors, J. Power Sources 175 (1) (2008) 675–679.
[90] G. Salitra, A. Soffer, L. Eliad, Y. Cohen, D. Aurbach, Carbon electrodes for double-layer capacitors I. Relations between ion and Pore dimensions, J. Electrochem. Soc. 147 (7) (2000) 2486–2493.
[91] C. Vix-Guterl, E. Frackowiak, K. Jurewicz, M. Friebe, J. Parmentier, F. Béguin, Electrochemical energy storage in ordered porous carbon materials, Carbon N. Y. 43 (6) (2005) 1293–1302.
[92] L. Eliad, G. Salitra, A. Soffer, D. Aurbach, On the mechanism of selective electroadsorption of protons in the pores of carbon molecular sieves, Langmuir 21 (7) (2005) 3198–3202.
[93] L. Eliad, E. Pollak, N. Levy, G. Salitra, A. Soffer, D. Aurbach, Assessing optimal pore-to-ion size relations in the design of porous poly(vinylidene chloride) carbons for EDL capacitors, Appl. Phys. A Mater. Sci. Process. 82 (4) (2006) 607–613.
[94] M. Arulepp, et al., The advanced carbide-derived carbon based supercapacitor, J. Power Sources 162 (2) (2006) 1460–1466.
[95] M. Arulepp, et al., Influence of the solvent properties on the characteristics of a double layer capacitor, J. Power Sources 133 (2) (2004) 320–328.
[96] E. Raymundo-Piñero, K. Kierzek, J. Machnikowski, F. Béguin, Relationship between the nanoporous texture of activated carbons and their capacitance properties in different electrolytes, Carbon N. Y. 44 (12) (2006) 2498–2507.
[97] A. Jänes, E. Lust, Electrochemical characteristics of nanoporous carbide-derived carbon materials in various nonaqueous electrolyte solutions, J. Electrochem. Soc. 153 (1) (2006) A113–A116.
[98] B.D. Shanina, et al., A study of nanoporous carbon obtained from ZC powders (Z = Si, Ti, and B), Carbon N. Y. 41 (15) (2003) 3027–3036.
[99] J. Chmiola, G. Yushin, R. Dash, Y. Gogotsi, Effect of pore size and surface area of carbide derived carbons on specific capacitance, J. Power Sources 158 (1) (2006) 765–772.
[100] R. Dash, et al., Titanium carbide derived nanoporous carbon for energy-related applications, Carbon N. Y. 44 (12) (2006) 2489–2497.
[101] S. Urbonaite, et al., EELS studies of carbide derived carbons, Carbon N. Y. 45 (10) (2007) 2047–2053.
[102] Y. Gogotsi, et al., Nanoporous carbide-derived carbon with tunable pore size, Nat. Mater. 2 (9) (2003) 591–594.
[103] J. Huang, B.G. Sumpter, V. Meunier, A universal model for nanoporous carbon supercapacitors applicable to diverse pore regimes, carbon materials, and electrolytes, Chem. - A Eur. J. 14 (22) (2008) 6614–6626.
[104] X. Du, et al., Preparation of activated carbon hollow fibers from ramie at low temperature for electric double-layer capacitor applications, Bioresour. Technol. 149 (2013) 31–37.
[105] S.K. Singh, V.M. Dhavale, R. Boukherroub, S. Kurungot, S. Szunerits, N-doped porous reduced graphene oxide as an efficient electrode material for high performance flexible solid-state supercapacitor, Appl. Mater. Today (2016).
[106] Z. Yu, L. Tetard, L. Zhai, J. Thomas, Supercapacitor electrode materials: nanostructures from 0 to 3 dimensions, Energy Environ. Sci. 8 (3) (2015) 702–730.
[107] Z.G. Cambaz, G.N. Yushin, Y. Gogotsi, K.L. Vyshnyakova, L.N. Pereselentseva, Formation of carbide-derived carbon on β-silicon carbide whiskers, J. Am. Ceram. Soc. 89 (2) (2006) 509–514.
[108] J.H. Chen, W.Z. Li, D.Z. Wang, S.X. Yang, J.G. Wen, Z.F. Ren, Electrochemical characterization of carbon nanotubes as electrode in electrochemical double-layer capacitors, Carbon N. Y. 40 (8) (2002) 1193–1197.
[109] S. Stankovich, et al., Graphene-based composite materials, Nature 442 (7100) (2006) 282–286.
[110] M. Seredych, T.J. Bandosz, Removal of ammonia by graphite oxide via its intercalation and reactive adsorption, Carbon N. Y. 45 (10) (2007) 2130–2132.
[111] S.R.C. Vivekchand, C.S. Rout, K.S. Subrahmanyam, A. Govindaraj, C.N.R. Rao, Graphene-based electrochemical supercapacitors, J. Chem. Sci. 120 (1) (2008) 9–13.
[112] Z.Y. Zhang, B.C. Sun, Z. Cao, Data extraction method for heterogeneous database based on EJB, Advanced Mat. Res. 756 (2013) 1408–1412.
[113] Y. Yoon, et al., Vertical alignments of graphene sheets spatially and densely piled for fast ion diffusion in compact supercapacitors, ACS Nano 8 (5) (2014) 4580–4590.
[114] D.T. Pham, et al., Carbon nanotube-bridged graphene 3D building blocks for ultrafast compact supercapacitors, ACS Nano 9 (2) (2015) 2018–2027.
[115] Y. Wang, et al., Supercapacitor devices based on graphene materials, J. Phys. Chem. C 113 (30) (2009) 13103–13107.
[116] Y. Yang, et al., Graphene-based materials with tailored nanostructures for energy conversion and storage, Mater. Sci. Eng. R Reports 102 (2016) 1–72.
[117] Q. Ke, J. Wang, Graphene-based materials for supercapacitor electrodes–A review, J. Mater. 2 (1) (2016) 37–54.
[118] P. Du, et al., Self-powered electronics by integration of flexible solid-state graphene-based supercapacitors with high performance perovskite hybrid solar cells, Adv. Funct. Mater. 25 (16) (2015) 2420–2427.
[119] Q. Ke, Y. Liu, H. Liu, Y. Zhang, Y. Hu, J. Wang, Surfactant-modified chemically reduced graphene oxide for electrochemical supercapacitors, RSC Adv. 4 (50) (2014) 26398–26406.
[120] Q. Cheng, J. Tang, J. Ma, H. Zhang, N. Shinya, L.-C. Qin, Graphene and carbon nanotube composite electrodes for supercapacitors with ultra-high energy density, Phys. Chem. Chem. Phys. 13 (39) (2011) 17615–17624.
[121] C. Zheng, X. Zhou, H. Cao, G. Wang, Z. Liu, Synthesis of porous graphene/activated carbon composite with high packing density and large specific surface area for supercapacitor electrode material, J. Power Sources 258 (2014) 290–296.
[122] Y. Cao, et al., Boosting supercapacitor performance of carbon fibres using electrochemically reduced graphene oxide additives, Phys. Chem. Chem. Phys. 15 (45) (2013) 19550–19556.
[123] J. Yan, Q. Wang, C. Lin, T. Wei, Z. Fan, Interconnected frameworks with a sandwiched porous carbon layer/graphene hybrids for supercapacitors with high gravimetric and volumetric performances, Adv. Energy Mater. 4 (13) (2014) 1400500.
[124] Y. Xu, Z. Lin, X. Huang, Y. Wang, Y. Huang, X. Duan, Functionalized graphene hydrogel-based high-performance supercapacitors, Adv. Mater. 25 (40) (2013) 5779–5784.
[125] N. An, Y. An, Z. Hu, B. Guo, Y. Yang, Z. Lei, Graphene hydrogels non-covalently functionalized with alizarin: an ideal electrode material for symmetric supercapacitors, J. Mater. Chem. A 3 (44) (2015) 22239–22246.
[126] G. Wang, et al., Flexible pillared graphene-paper electrodes for high-performance electrochemical supercapacitors, Small 8 (3) (2012) 452–459.
[127] D.P. Dubal, Electrochemistry, [Online]. Available: https://www.tu-chemnitz.de/chemie/elchem/projekte/dubal.php . [Accessed: 17-Jul (2017).
[128] Z. Zeng, H. Zhou, X. Long, E. Guo, X. Wang, Electrodeposition of hierarchical manganese oxide on metal nanoparticles decorated nanoporous gold with enhanced supercapacitor performance, J. Alloys Compd. 632 (2015) 376–385.
[129] C.C. Hu, W.C. Chen, Effects of substrates on the capacitive performance of RuO x.nH2O and activated carbon-RuOx electrodes for supercapacitors, Electrochim. Acta 49 (21) (2004) 3469–3477.
[130] J.R. Miller, P. Simon, Materials science: electrochemical capacitors for energy management, Science (80-.) 321 (5889) (2008) 651–652.
[131] K. Sakiyama, et al., Deposition and properties of reactively sputtered ruthenium dioxide films, J. Electrochem. Soc. 140 (3) (1993) 834–839.
[132] H. Lee, M.S. Cho, I.H. Kim, J. Do Nam, Y. Lee, RuOx/polypyrrole nanocomposite electrode for electrochemical capacitors, Synth. Met. 160 (9–10) (2010) 1055–1059.
[133] J.P. Zheng, P.J. Cygan, T.R. Jow, Hydrous ruthenium oxide as an electrode material for electrochemical capacitors, J. Electrochem. Soc. 142 (8) (1995) 2699–2703.
[134] N.L. Wu, S.L. Kuo, M.H. Lee, Preparation and optimization of RuO2-impregnated SnO2 xerogel supercapacitor, J. Power Sources 104 (1) (2002) 62–65.
[135] Y.R. Ahn, M.Y. Song, S.M. Jo, C.R. Park, D.Y. Kim, Electrochemical capacitors based on electrodeposited ruthenium oxide on nanofibre substrates, Nanotechnology 17 (12) (2006) 2865–2869.
[136] J.N. Broughton, M.J. Brett, Investigation of thin sputtered Mn films for electrochemical capacitors, Electrochim. Acta 49 (25) (2004) 4439–4446.
[137] C.C. Hu, T.W. Tsou, Ideal capacitive behavior of hydrous manganese oxide prepared by anodic deposition, Electrochem. commun. 4 (2) (2002) 105–109.
[138] S.-F. Chin, S.-C. Pang, M.A. Anderson, Material and electrochemical characterization of tetrapropylammonium manganese oxide thin films as novel electrode materials for electrochemical capacitors, J. Electrochem. Soc. 149 (4) (2002) A379–A384.
[139] K. Shi, M. Ren, I. Zhitomirsky, Activated carbon-coated carbon nanotubes for

energy storage in supercapacitors and capacitive water purification, ACS Sustain. Chem. Eng. 2 (5) (2014) 1289–1298.
[140] K. Shi, I. Zhitomirsky, Asymmetric supercapacitors based on activated-carbon--coated carbon nanotubes, ChemElectroChem 2 (3) (2015) 396–403.
[141] Y. Zhu, Z. Wu, M. Jing, X. Yang, W. Song, X. Ji, Mesoporous NiCo2S4 nanoparticles as high-performance electrode materials for supercapacitors, J. Power Sources 273 (2015) 584–590.
[142] Q. Wang, et al., NiCo2O4 nanowire arrays supported on Ni foam for high-performance flexible all-solid-state supercapacitors, J. Mater. Chem. A 1 (7) (2013) 2468–2473.
[143] J. Seetharamappa, S. Yellappa, F. D'Souza, Carbon nanotubes: next generation of electronic material, Electrochem. Soc. Interface 15 (2) (2006) 23–26.
[144] H.B. Li, et al., Amorphous nickel hydroxide nanospheres with ultrahigh capacitance and energy density as electrochemical pseudocapacitor materials, Nat. Commun. 4 (1–7) (2013) 1894.
[145] X.F. Wang, Z. You, D.B. Ruan, A hybrid metal oxide supercapacitor in aqueous KOH electrolyte, Chinese J. Chem. 24 (9) (2006) 1126–1132.
[146] C. Lin, J.A. Ritter, B.N. Popov, Characterization of sol-gel-derived cobalt oxide xerogels as electrochemical capacitors, J. Electrochem. Soc. 145 (12) (1998) 4097–4103.
[147] T. Wen, C. Hu, Y. Li, The redox behavior of electroless Ni/PTFE deposits in KOH, J. Electrochem. Soc. 140 (9) (1993) 2554–2558.
[148] D.D. Zhao, S.J. Bao, W.J. Zhou, H.L. Li, Preparation of hexagonal nanoporous nickel hydroxide film and its application for electrochemical capacitor, Electrochem. commun. 9 (5) (2007) 869–874.
[149] M. Wu, J. Gao, S. Zhang, A. Chen, Comparative studies of nickel oxide films on different substrates for electrochemical supercapacitors, J. Power Sources 159 (1) (2006) 365–369.
[150] H. Kuan-Xin, W. Quan-Fu, Z. Xiao-gang, W. Xin-Lei, Electrodeposition of nickel and cobalt mixed Oxide/Carbon nanotube thin films and their charge storage properties, J. Electrochem. Soc. 153 (8) (2006) A1568–A1574.
[151] T. Brousse, D. Bélanger, J.W. Long, to Be or not to Be pseudocapacitive? J. Electrochem. Soc. 162 (5) (2015) A5185–A5189.
[152] Y. Gogotsi, What nano can do for energy storage, ACS Nano 8 (6) (2014) 5369–5371.
[153] Y. Gogotsi, P. Simon, True performance metrics in electrochemical energy storage, Science (80-.). 334 (6058) (2011) 917–918.
[154] P. Simon, Y. Gogotsi, B. Dunn, Where do batteries end and supercapacitors begin? Science (80-.) 343 (6176) (2014) 1210–1211.
[155] K. Rajendra Prasad, N. Miura, Electrochemical synthesis and characterization of nanostructured tin oxide for electrochemical redox supercapacitors, Electrochem. commun. 6 (8) (2004) 849–852.
[156] S.-L. Kuo, N.-L. Wu, Composite supercapacitor containing tin oxide and electroplated ruthenium oxide, Electrochem. solid-state Lett. 6 (5) (2003) A85–A87.
[157] W. Dong, J.S. Sakamoto, B. Dunn, Electrochemical properties of vanadium oxide aerogels, Sci. Technol. Adv. Mater. 4 (1) (2003) 3–11.
[158] H.Y. Lee, J.B. Goodenough, Ideal supercapacitor behavior of amorphous V2O5·nH2O in potassium chloride (KCl) aqueous solution, J. Solid State Chem. 148 (1) (1999) 81–84.
[159] I.-H. Kim, J.-H. Kim, B.-W. Cho, Y.-H. Lee, K.-B. Kim, Synthesis and electrochemical characterization of vanadium oxide on carbon nanotube film substrate for pseudocapacitor applications, J. Electrochem. Soc. 153 (6) (2006) A989–A996.
[160] K.R. Prasad, K. Koga, N. Miura, Electrochemical deposition of nanostructured indium oxide: high-performance electrode material for redox supercapacitors, Chem. Mater. 16 (10) (2004) 1845–1847.
[161] T.P. Gujar, V.R. Shinde, C.D. Lokhande, S.H. Han, Electrosynthesis of Bi2O3 thin films and their use in electrochemical supercapacitors, J. Power Sources 161 (2) (2006) 1479–1485.
[162] S.-Y. Wang, K.-C. Ho, S.-L. Kuo, N.-L. Wu, Investigation on capacitance mechanisms of Fe3O4 electrochemical capacitors, J. Electrochem. Soc. 153 (1) (2006) A75–A80.
[163] S.L. Kuo, N.L. Wu, Electrochemical characterization on MnFe2O4/carbon black composite aqueous supercapacitors, J. Power Sources 162 (2) (2006) 1437–1443.
[164] S.-L. Kuo, N.-L. Wu, Electrochemical capacitor of MnFe2O4 with NaCl electrolyte, Electrochem. Solid-State Lett. 8 (10) (2005) A495–A499.
[165] J.L. Gunjakar, A.M. More, V.R. Shinde, C.D. Lokhande, Synthesis of nanocrystalline nickel ferrite (NiFe2O4) thin films using low temperature modified chemical method, J. Alloys Compd. 465 (1–2) (2008) 468–473.
[166] J.H. Jang, A. Kato, K. Machida, K. Naoi, Supercapacitor performance of hydrous ruthenium oxide electrodes prepared by electrophoretic deposition, J. Electrochem. Soc. 153 (2) (2006) A321–A328.
[167] S.C. Pang, M.A. Anderson, T.W. Chapman, Novel electrode materials for thin-film ultracapacitors: comparison of electrochemical properties of sol-gel-derived and electrodeposited manganese dioxide, J. Electrochem. Soc. 147 (2) (2000) 444–450.
[168] G.A.M. Ali, O.A.G. Wahba, A.M. Hassan, O.A. Fouad, K. Feng Chong, Calcium-based nanosized mixed metal oxides for supercapacitor application, Ceram. Int. 41 (6) (2015) 8230–8234.
[169] Y. Tang, et al., Morphology controlled synthesis of monodisperse cobalt hydroxide for supercapacitor with high performance and long cycle life, J. Power Sources 256 (2014) 160–169.
[170] B. Bhujun, M.T.T. Tan, A.S. Shanmugam, Evaluation of aluminium doped spinel ferrite electrodes for supercapacitors, Ceram. Int. 42 (5) (2016) 6457–6466.
[171] A.R. De Souza, E. Arashiro, H. Golveia, T.A.F. Lassali, Pseudocapacitive behavior of Ti/RhOx + Co3O4 electrodes in acidic medium: application to supercapacitor development, Electrochim. Acta 49 (12) (2004) 2015–2023.
[172] K. Li, Ceramic Membranes for Separation and Reaction, John Wiley and Sons, 2007.
[173] Y. Cao, B. Lin, Y. Sun, H. Yang, X. Zhang, Structure, morphology and electrochemical properties of LaxSr1 - xCo0.1Mn0.9O3 - δ perovskite nanofibers prepared by electrospinning method, J. Alloys Compd. 624 (2015) 31–39.
[174] X. Lang, H. Mo, X. Hu, H. Tian, Supercapacitor performance of perovskite $La_{1-x}Sr_xMnO_3$, Dalt. Trans. 46 (40) (2017) 13720–13730.
[175] P.M. Wilde, T.J. Guther, R. Oesten, J. Garche, Strontium ruthenate perovskite as the active material for supercapacitors, J. Electroanal. Chem. 461 (1–2) (1999) 154–160.
[176] M. Wohlfahrt-Mehrens, J. Schenk, P.M. Wilde, E. Abdelmula, P. Axmann, J. Garche, New materials for supercapacitors, J. Power Sources 105 (2) (2002) 182–188.
[177] C. Balamurugan, S. Arunkumar, D.W. Lee, Hierarchical 3D nanostructure of GdInO3 and reduced-graphene-decorated GdInO3 nanocomposite for CO sensing applications, Sensors Actuators, B Chem. 234 (2016) 155–166.
[178] A. Rai, A.L. Sharma, A.K. Thakur, Evaluation of aluminium doped lanthanum ferrite based electrodes for supercapacitor design, Solid State Ionics 262 (2014) 230–233.
[179] J.H. Ji, J.W. Lee, H. Chung, J.H. Koh, (Na,K)NbO3-CaCu3Ti4O12 perovskite composites for supercapacitor based piezoelectric devices, Ceram. Int. 42 (2016) 4978–4983.
[180] C.D. Lokhande, T.P. Gujar, V.R. Shinde, R.S. Mane, S.H. Han, Electrochemical supercapacitor application of pervoskite thin films, Electrochem. commun. 9 (7) (2007) 1805–1809.
[181] D.K. Hwang, S. Kim, J.-H. Lee, I.-S. Hwang, I.-D. Kim, Phase evolution of perovskite LaNiO3 nanofibers for supercapacitor application and p-type gas sensing properties of LaOCl–NiO composite nanofibers, J. Mater. Chem. 21 (6) (2011) 1959–1965.
[182] Y. Cao, B. Lin, Y. Sun, H. Yang, X. Zhang, Synthesis, structure and electrochemical properties of lanthanum manganese nanofibers doped with Sr and Cu, J. Alloys Compd. 638 (2015) 204–213.
[183] Y. Cao, B. Lin, Y. Sun, H. Yang, X. Zhang, Sr-doped lanthanum nickelate nanofibers for high energy density supercapacitors, Electrochim. Acta 174 (1) (2015) 41–50.
[184] Y. Cao, B. Lin, Y. Sun, H. Yang, X. Zhang, Symmetric/Asymmetric supercapacitor based on the perovskite-type lanthanum cobaltate nanofibers with Sr-substitution, Electrochim. Acta 178 (2015) 398–406.
[185] J. Hu, J. Men, J. Ma, H. Huang, Preparation of LaMnO3/graphene thin films and their photocatalytic activity, J. Rare Earths 32 (12) (2014) 1126–1134.
[186] K. Ahmad, A. Mohammad, P. Mathur, S.M. Mobin, Preparation of SrTiO3 perovskite decorated rGO and electrochemical detection of nitroaromatics, Electrochim. Acta (2016).
[187] N. Arjun, G.T. Pan, T.C.K. Yang, The exploration of lanthanum based perovskites and their complementary electrolytes for the supercapacitor applications, Results Phys. 7 (2017) 920–926.
[188] L. Zhu, Y. Liu, C. Su, W. Zhou, M. Liu, Z. Shao, Perovskite SrCo0.9Nb0.1O3-δ as an anion-intercalated electrode material for supercapacitors with ultrahigh volumetric energy density, Angew. Chemie - Int. Ed. 55 (33) (2016) 9576–9579.
[189] J. Lv, et al., Strontium doped lanthanum manganite/manganese dioxide composite electrode for supercapacitor with enhanced rate capability, Electrochim. Acta 222 (2016) 1585–1591.
[190] X.W. Wang, Q.Q. Zhu, X.E. Wang, H.C. Zhang, J.J. Zhang, L.F. Wang, Structural and electrochemical properties of La0.85Sr0.15MnO3 powder as an electrode material for supercapacitor, J. Alloys Compd. 675 (2016) 195–200.
[191] D.S. Dhawale, A. Vinu, C.D. Lokhande, Stable nanostructured polyaniline electrode for supercapacitor application, Electrochim. Acta 56 (25) (2011) 9482–9487.
[192] G. Inzelt, Conducting Polymers: a New Era in Electrochemistry, Springer Science & Business Media, 2012.
[193] H. Kuang, Q. Cao, X. Wang, B. Jing, Q. Wang, L. Zhou, Influence of the reaction temperature on polyaniline morphology and evaluation of their performance as supercapacitor electrode, J. Appl. Polym. Sci. 130 (5) (2013) 3753–3758.
[194] S. Grover, S. Goel, R.B. Marichi, V. Sahu, G. Singh, R.K. Sharma, Polyaniline all solid-State pseudocapacitor: role of morphological variations in performance evolution, Electrochim. Acta 196 (2016) 131–139.
[195] S.C. Huang, S.M. Huang, H. Ng, R.B. Kaner, Polyaniline capacitors, Synth. Met. 57 (1) (1993) 4047–4052.
[196] A. Rudge, I. Raistrick, S. Gottesfeld, J.P. Ferraris, A study of the electrochemical properties of conducting polymers for application in electrochemical capacitors, Electrochim. Acta 39 (2) (1994) 273–287.
[197] C. Arbizzani, M. Mastragostino, L. Meneghello, Polymer-based redox supercapacitors: a comparative study, Electrochim. Acta 41 (1) (1996) 21–26.
[198] C. Bian, A. Yu, De-doped polyaniline nanofibres with micropores for high-rate aqueous electrochemical capacitor, Synth. Met. 160 (13–14) (2010) 1579–1583.
[199] V. Sharma, A. Sahoo, Y. Sharma, P. Mohanty, Synthesis of nanoporous hypercrosslinked polyaniline (HCPANI) for gas sorption and electrochemical supercapacitor applications, RSC Adv. 5 (57) (2015) 45749–45754.
[200] H. Zhang, H. Li, F. Zhang, J. Wang, Z. Wang, S. Wang, Polyaniline nanofibers prepared by a facile electrochemical approach and their supercapacitor performance, J. Mater. Res. 23 (9) (2008) 2326–2332.
[201] L.Z. Fan, Y.S. Hu, J. Maier, P. Adelhelm, B. Smarsly, M. Antonietti, High electroactivity of polyaniline in supercapacitors by using a hierarchically porous carbon monolith as a support, Adv. Funct. Mater. 17 (16) (2007) 3083–3087.
[202] V. Gupta, N. Miura, Polyaniline/single-wall carbon nanotube (PANI/SWCNT) composites for high performance supercapacitors, Electrochim. Acta 52 (4) (2006) 1721–1726.

[203] S. He, X. Hu, S. Chen, H. Hu, M. Hanif, H. Hou, Needle-like polyaniline nanowires on graphite nanofibers: hierarchical micro/nano-architecture for high performance supercapacitors, J. Mater. Chem. 22 (11) (2012) 5114–5120.
[204] Y. Li, X. Zhao, P. Yu, Q. Zhang, Oriented arrays of polyaniline nanorods grown on graphite nanosheets for an electrochemical supercapacitor, Langmuir 29 (1) (2013) 493–500.
[205] Y.Y. Horng, Y.C. Lu, Y.K. Hsu, C.C. Chen, L.C. Chen, K.H. Chen, Flexible supercapacitor based on polyaniline nanowires/carbon cloth with both high gravimetric and area-normalized capacitance, J. Power Sources 195 (13) (2010) 4418–4422.
[206] K.R. Prasad, N. Miura, Polyaniline-MnO2 composite electrode for high energy density electrochemical capacitor, Electrochem. solid-state Lett. 7 (11) (2004) A425–A428.
[207] T. Takei, N. Muraki, N. Xu, A. Miura, N. Kumada, Anodic hybridization of fluorinated layered perovskite nanosheet with polyaniline for electrochemical capacitor, Colloids Surfaces A Physicochem. Eng. Asp. 459 (2014) 186–193.
[208] X. Xia, Q. Hao, W. Lei, W. Wang, D. Sun, X. Wang, Nanostructured ternary composites of graphene/Fe 2O 3/polyaniline for high-performance supercapacitors, J. Mater. Chem. 22 (33) (2012) 16844–16850.
[209] S. Giri, D. Ghosh, C.K. Das, Growth of vertically aligned tunable polyaniline on graphene/ZrO2 nanocomposites for supercapacitor energy-storage application, Adv. Funct. Mater. 24 (9) (2014) 1312–1324.
[210] C. Zhou, Y. Zhang, Y. Li, J. Liu, Construction of high-capacitance 3D CoO@ Polypyrrole nanowire array electrode for aqueous asymmetric supercapacitor, Nano Lett. 13 (5) (2013) 2078–2085.
[211] X.H. Xia, et al., Multicolor and fast electrochromism of nanoporous NiO/poly(3,4-ethylenedioxythiophene) composite thin film, Electrochem. commun. 11 (3) (2009) 702–705.
[212] M. Liu, et al., Hierarchical composites of polyaniline-graphene nanoribbons-carbon nanotubes as electrode materials in all-solid-state supercapacitors, Nanoscale 5 (16) (2013) 7312–7320.
[213] K. Rajendra Prasad, N. Munichandraiah, Electrochemical studies of polyaniline in a gel polymer electrolyte: High energy and high power characteristics of a solid-state redox supercapacitor, Electrochem. Solid-State Lett. 5 (12) (2002) A271–A274.
[214] V. Gupta, N. Miura, Electrochemically deposited polyaniline nanowire's network a high-performance electrode material for redox supercapacitor, Electrochem. Solid-State Lett. 8 (12) (2005) A630–A632.
[215] K. Wang, J. Huang, Z. Wei, Conducting polyaniline nanowire arrays for high performance supercapacitors, J. Phys. Chem. C 114 (17) (2010) 8062–8067.
[216] P. Bandyopadhyay, T. Kuila, J. Balamurugan, T.T. Nguyen, N.H. Kim, J.H. Lee, Facile synthesis of novel sulfonated polyaniline functionalized graphene using m-aminobenzene sulfonic acid for asymmetric supercapacitor application, Chem. Eng. J. 308 (2017) 1174–1184.
[217] D. Bélanger, et al., Characterization and long-term performance of polyaniline-based electrochemical capacitors, J. Electrochem. Soc. 147 (8) (2000) 2923–2929.
[218] M.A. Bavio, G.G. Acosta, T. Kessler, Polyaniline and polyaniline-carbon black nanostructures as electrochemical capacitor electrode materials, Int. J. Hydrogen Energy 39 (16) (2014) 8582–8589.
[219] P. Yu, X. Zhao, Z. Huang, Y. Li, Q. Zhang, Free-standing three-dimensional graphene and polyaniline nanowire arrays hybrid foams for high-performance flexible and lightweight supercapacitors, J. Mater. Chem. A 2 (35) (2014) 14413–14420.
[220] B. Song, F. Wu, Y. Zhu, Z. Hou, K. sik Moon, C.P. Wong, Effect of polymer binders on graphene-based free-standing electrodes for supercapacitors, Electrochim. Acta 267 (2018) 213–221.
[221] Z. Zhu, et al., Effects of various binders on supercapacitor performances, Int. J. Electrochem. Sci. 11 (10) (2016) 8270–8279.
[222] D. Bresser, D. Buchholz, A. Moretti, A. Varzi, S. Passerini, Alternative binders for sustainable electrochemical energy storage-the transition to aqueous electrode processing and bio-derived polymers, Energy Environ. Sci. 11 (11) (2018) 3096–3127.
[223] A. Balducci, U. Bardi, S. Caporali, M. Mastragostino, F. Soavi, Ionic liquids for hybrid supercapacitors, Electrochem. commun. 6 (6) (2004) 566–570.
[224] N. Choudhury, S. Sampath, A.K. Shukla, Hydrogel-polymer electrolytes for electrochemical capacitors: an overview, Energy Environ. Sci. 2 (1) (2009) 55–67.
[225] H. Gao, K. Lian, Proton-conducting polymer electrolytes and their applications in solid supercapacitors: a review, RSC Adv. 4 (62) (2014) 33091–33113.
[226] C. Zhong, Y. Deng, W. Hu, J. Qiao, L. Zhang, J. Zhang, A review of electrolyte materials and compositions for electrochemical supercapacitors, Chem. Soc. Rev. 44 (21) (2015) 7484–7539.
[227] a B. Samui, P. Sivaraman, Solid polymer electrolytes for supercapacitors, Polymer Electrolytes: Fundamentals and Applications, (2010), pp. 431–470.
[228] C. Masarapu, L.P. Wang, X. Li, B. Wei, Tailoring electrode/electrolyte interfacial properties in flexible supercapacitors by applying pressure, Adv. Energy Mater. 2 (5) (2012) 546–552.
[229] C. Long, T. Wei, J. Yan, L. Jiang, Z. Fan, Supercapacitors based on graphene-supported iron nanosheets as negative electrode materials, ACS Nano 7 (12) (2013) 11325–11332.
[230] C.Z. Yuan, B. Gao, X.G. Zhang, Electrochemical capacitance of NiO/Ru0.35V0.65O2 asymmetric electrochemical capacitor, J. Power Sources 173 (1) (2007) 606–612.
[231] C.H. Wang, H.C. Hsu, J.H. Hu, High-energy asymmetric supercapacitor based on petal-shaped MnO2 nanosheet and carbon nanotube-embedded polyacrylonitrile-based carbon nanofiber working at 2 v in aqueous neutral electrolyte, J. Power Sources 249 (2014) 1–8.
[232] D.E. Jiang, J. Wu, Microscopic insights into the electrochemical behavior of nonaqueous electrolytes in electric double-layer capacitors, J. Phys. Chem. Lett. 4 (8) (2013) 1260–1267.
[233] J.S. Bonso, et al., Exfoliated graphite nanoplatelets-V2O5 nanotube composite electrodes for supercapacitors, J. Power Sources 203 (2012) 227–232.
[234] C. Arbizzani, M. Mastragostino, F. Soavi, New trends in electrochemical supercapacitors, J. Power Sources 100 (1–2) (2001) 164–170.
[235] Y. Mun, et al., Simple synthesis of hierarchically structured partially graphitized carbon by emulsion/block-copolymer co-template method for high power supercapacitors, Carbon N. Y. 64 (2013) 391–402.
[236] M. Jana, P. Khanra, N.C. Murmu, P. Samanta, J.H. Lee, T. Kuila, Covalent surface modification of chemically derived graphene and its application as supercapacitor electrode material, Phys. Chem. Chem. Phys. 16 (16) (2014) 7618–7626.
[237] X. Liu, et al., Three-dimensional and stable polyaniline-grafted graphene hybrid materials for supercapacitor electrodes, J. Mater. Chem. A 2 (37) (2014) 15273–15278.
[238] B.S. Mao, Z. Wen, Z. Bo, J. Chang, X. Huang, J. Chen, Hierarchical nanohybrids with porous CNT-networks decorated crumpled graphene balls for supercapacitors, ACS Appl. Mater. Interfaces 6 (12) (2014) 9881–9889.
[239] L. Li, et al., Electrospun porous NiCo2O4 nanotubes as advanced electrodes for electrochemical capacitors, Chem. - A Eur. J. 19 (19) (2013) 5892–5898.
[240] S. Dhibar, P. Bhattacharya, G. Hatui, S. Sahoo, C.K. Das, Transition metal-doped polyaniline/single-walled carbon nanotubes nanocomposites: efficient electrode material for high performance supercapacitors, ACS Sustain. Chem. Eng. 2 (5) (2014) 1114–1127.
[241] S. Li, L. Qi, L. Lu, H. Wang, Facile preparation and performance of mesoporous manganese oxide for supercapacitors utilizing neutral aqueous electrolytes, RSC Adv. 2 (8) (2012) 3298–3308.
[242] H. Xia, Y.S. Meng, G. Yuan, C. Cui, L. Lu, A symmetric RuO2/RuO2 supercapacitor operating at 1.6 v by using a neutral aqueous electrolyte, Electrochem. Solid-State Lett. 15 (4) (2012) A60–A63.
[243] M. Sevilla, A.B. Fuertes, Direct synthesis of highly porous interconnected carbon nanosheets and their application as high-performance supercapacitors, ACS Nano 8 (5) (2014) 5069–5078.
[244] Y. Lai, X. Chen, Z. Zhang, J. Li, Y. Liu, Tetraethylammonium difluoro(oxalato) borate as electrolyte salt for electrochemical double-layer capacitors, Electrochim. Acta 56 (18) (2011) 6426–6430.
[245] W. Qian, et al., Human hair-derived carbon flakes for electrochemical supercapacitors, Energy Environ. Sci. 7 (1) (2013) 379–386.
[246] D. Yiğit, M. Güllü, T. Yumak, A. Sınağ, Heterostructured poly (3, 6-dithien-2-yl-9 H-carbazol-9-yl acetic acid)/TiO 2 nanoparticles composite redox-active materials as both anode and cathode for high-performance symmetric supercapacitor applications, J. Mater. Chem. A 2 (18) (2014) 6512–6524.
[247] S.D. Perera, et al., Manganese oxide nanorod-graphene/vanadium oxide nanowire-graphene binder-free paper electrodes for metal oxide hybrid supercapacitors, Nano Energy 2 (5) (2013) 966–975.
[248] X. Liu, et al., A NiAl layered double hydroxide@carbon nanoparticles hybrid electrode for high-performance asymmetric supercapacitors, J. Mater. Chem. A 2 (2014) 1682–1685.
[249] X. Yang, K. Xu, R. Zou, J. Hu, A hybrid electrode of Co3O4@ PPy core/shell nanosheet arrays for high-performance supercapacitors, Nano-Micro Lett. 8 (2) (2016) 143–150.
[250] Y. Cai, B. Zhao, J. Wang, Z. Shao, Non-aqueous hybrid supercapacitors fabricated with mesoporous TiO2 microspheres and activated carbon electrodes with superior performance, J. Power Sources 253 (2014) 80–89.
[251] E. Lim, et al., High-performance sodium-ion hybrid supercapacitor based on Nb2O5@Carbon Core–Shell nanoparticles and reduced graphene oxide nanocomposites, Adv. Funct. Mater. 26 (21) (2016) 3711–3719.
[252] X. Yun, J. Li, Z. Luo, J. Tang, Y. Zhu, Advanced aqueous energy storage devices based on flower-like nanosheets-assembled Ni0.85Se microspheres and porous Fe2O3 nanospheres, Electrochim. Acta 302 (2019) 449–458.
[253] Lithium-ion capacitor, Wikipedia. [Online]. Available: http://www.wikiwand.com/en/Lithium-ion_capacitor. [Accessed: 03-Jul-2017].
[254] M.S. Halper, J.C. Ellenbogen, Supercapacitors: A Brief Overview, MITRE Nanosyst. Gr., 2006.
[255] D. Cericola, R. Kötz, Hybridization of rechargeable batteries and electrochemical capacitors: principles and limits, Electrochim. Acta (2012) 1–17.
[256] A. Laforgue, et al., Activated carbon/conducting polymer hybrid supercapacitors, J. Electrochem. Soc. 150 (5) (2003) A645–A651.
[257] Y. Shao, et al., Design and mechanisms of asymmetric supercapacitors, Chem. Rev. 118 (18) (2018) 9233–9280.
[258] Y. Zhu, et al., Porous NiCo2O4 spheres tuned through carbon quantum dots utilised as advanced materials for an asymmetric supercapacitor, J. Mater. Chem. A 3 (2) (2015) 866–877.
[259] W.G. Pell, B.E. Conway, Peculiarities and requirements of asymmetric capacitor devices based on combination of capacitor and battery-type electrodes, J. Power Sources 136 (2) (2004) 1–17 (Special issue).
[260] Y. Zhu, Z. Huang, Z. Hu, L. Xi, X. Ji, Y. Liu, 3D interconnected ultrathin cobalt selenide nanosheets as cathode materials for hybrid supercapacitors, Electrochim. Acta 269 (2018) 30–37.
[261] W. Xue, W. Wang, Y. Fu, D. He, F. Zeng, R. Zhao, Rational synthesis of honeycomb-like NiCo2O4@ NiMoO4 core/shell nanofilm arrays on Ni foam for high-performance supercapacitors, Mater. Lett. 186 (2017) 34–37.
[262] A.A. Alguail, Battery Type Hybrid Supercapacitor Based on Conducting Polymers, Univerzitet u Beogradu-Tehnološko-metalurški fakultet, 2017, pp. 1–112.
[263] W.H. Low, P.S. Khiew, S.S. Lim, C.W. Siong, C.H. Chia, E.R. Ezeigwe, Facile synthesis of graphene-Zn3V2O8 nanocomposite as a high performance electrode

material for symmetric supercapacitor, J. Alloys Compd. 784 (2019) 847–858.
[264] P. Gómez-Romero, et al., Hybrid organic-inorganic nanocomposite materials for application in solid state electrochemical supercapacitors, Electrochem. commun. 5 (2) (2003) 149–153.
[265] A. Du Pasquier, I. Plitz, J. Gural, S. Menocal, G. Amatucci, Characteristics and performance of 500 F asymmetric hybrid advanced supercapacitor prototypes, J. Power Sources 113 (1) (2003) 62–71.
[266] M.F. El-Kady, et al., Engineering three-dimensional hybrid supercapacitors and microsupercapacitors for high-performance integrated energy storage, Proc. Natl. Acad. Sci. 112 (14) (2015) 4233–4238.
[267] E. Lim, et al., Advanced hybrid supercapacitor based on a mesoporous niobium pentoxide/carbon as high-performance anode, ACS Nano 8 (9) (2014) 8968–8978.
[268] J.H. Kim, H.J. Choi, H.K. Kim, S.H. Lee, Y.H. Lee, A hybrid supercapacitor fabricated with an activated carbon as cathode and an urchin-like TiO2 as anode, Int. J. Hydrogen Energy 41 (31) (2016) 13549–13556.
[269] H.J. Choi, J.H. Kim, H.K. Kim, S.H. Lee, Y.H. Lee, Improving the electrochemical performance of hybrid supercapacitor using Well-organized urchin-like TiO2 and activated carbon, Electrochim. Acta 208 (2016) 202–210.
[270] Y. He, et al., Freestanding three-dimensional graphene/MnO2 composite networks as ultralight and flexible supercapacitor electrodes, ACS Nano 7 (1) (2012) 174–182.
[271] F. Zhang, et al., A high-performance supercapacitor-battery hybrid energy storage device based on graphene-enhanced electrode materials with ultrahigh energy density, Energy Environ. Sci. 6 (5) (2013) 1623–1632.
[272] M. Zhou, Y. Deng, K. Liang, X. Liu, B. Wei, W. Hu, One-step route synthesis of active carbon@La2NiO4/NiO hybrid coatings as supercapacitor electrode materials: significant improvements in electrochemical performance, J. Electroanal. Chem. 742 (2015) 1–7.
[273] L.C. Gou Jianxia, Xie Shengli, Hollow sphere NiS2 as high-performance hybrid supercapacitor electrode materials, AIP Conf. Proc. 1794 (1) (2017) 020040 (1–4).
[274] G. Ma, et al., High-performance hybrid supercapacitor based on graphene-wrapped mesoporous T-Nb2O5 nanospheres anode and mesoporous carbon-coated graphene cathode, ChemElectroChem 3 (9) (2016) 1360–1368.
[275] S.Z.S.H. Kiamahalleh Meisam Valizadeh, Mat Sot Mohd Aimzi, Najafpour Ghasem, Optimization of specific capacitance for hybrid supercapacitor material based on nickel-manganese oxidesmultiwalled carbon NanotubesPoly (3, 4-ethylenedioxythiophene) using response surface methodology, World Appl. Sci. J. 9 (2010) 14–20 no. Special Issue of Carbon Nanotubes.
[276] A. Vlad, N. Singh, J. Rolland, S. Melinte, P.M. Ajayan, J.-F. Gohy, Hybrid supercapacitor-battery materials for fast electrochemical charge storage, Sci. Rep. 4 (1–7) (2014) 4315.
[277] X. Cao, et al., Preparation of novel 3D graphene networks for supercapacitor applications, Small 7 (22) (2011) 3163–3168.
[278] T. Hibino, K. Kobayashi, M. Nagao, S. Kawasaki, High-temperature supercapacitor with a proton-conducting metal pyrophosphate electrolyte, Sci. Rep. (2015) 1–7.
[279] X.C. Dong, et al., 3D graphene-cobalt oxide electrode for high-performance supercapacitor and enzymeless glucose detection, ACS Nano 6 (4) (2012) 3206–3213.
[280] S. Wang, et al., Free-standing 3D graphene/polyaniline composite film electrodes for high-performance supercapacitors, J. Power Sources 299 (2015) 347–355.
[281] T. Lee, T. Yun, B. Park, B. Sharma, H.-K. Song, B.-S. Kim, Hybrid multilayer thin film supercapacitor of graphene nanosheets with polyaniline: importance of establishing intimate electronic contact through nanoscale blending, J. Mater. Chem. 22 (39) (2012) 21092e–21099e.
[282] P. Yu, Y. Li, X. Zhao, L. Wu, Q. Zhang, Graphene-wrapped polyaniline nanowire arrays on nitrogen-doped carbon fabric as novel flexible hybrid electrode materials for High-performance supercapacitor, Langmuir 30 (18) (2014) 5306–5313.
[283] C.-Y. Chen, C.-Y. Fan, M.-T. Lee, J.-K. Chang, Tightly connected MnO2–graphene with tunable energy density and power density for supercapacitor applications, J. Mater. Chem. 22 (2012) 7697–7700.
[284] M.A.B.M. Sot, M.V. Kiamahalleh, G. Najafpour, Optimization of specific capacitance for hybrid supercapacitor material based on nickel-manganese Oxides/multivalled carbon Nanotubes/Poly (3, 4-ethylenedioxythiophene) using response surface methodology, World Appl. Sci. J. 9 (10) (2010) 14–20 no. (Special Issue of Carbon Nanotubes).
[285] Z.S. Wu, et al., Anchoring hydrous RuO2 on graphene sheets for high-performance electrochemical capacitors, Adv. Funct. Mater. 20 (20) (2010) 3595–3602.
[286] C. Xiang, M. Li, M. Zhi, A. Manivannan, N. Wu, A reduced graphene oxide/Co3O4 composite for supercapacitor electrode, J. Power Sources 226 (2013) 65–70.
[287] X. Xia, et al., Graphene sheet/porous NiO hybrid film for supercapacitor applications, Chem. - A Eur. J. 17 (39) (2011) 10898–10905.
[288] M. Li, G. Sun, P. Yin, C. Ruan, K. Ai, Controlling the formation of rodlike V2O5 nanocrystals on reduced graphene oxide for high-performance supercapacitors, ACS Appl. Mater. Interfaces 5 (21) (2013) 11462–11470.
[289] D.M. Zogbi, The Global Supercapacitor Market Is Facing Unique Challenges in 2016, TTI, Inc, 2016 [Online]. Available: http://www.ttieurope.com/object/mezogbi-20161003.html . [Accessed: 20-Jul-2017].
[290] S. Chin, Supercapacitor Market Projected to Grow from $684.7 Million in 2016 to Over $2 Billion by 2022, (2017).
[291] F. Gonzalez, Supercapacitor Technologies and Markets 2016-2026, IDTechEx, 2017 [Online]. Available: http://www.idtechex.com/research/reports/supercapacitor-technologies-and-markets-2016-2026-000486.asp . [Accessed: 21-Jul-2017].
[292] B. Zhao, et al., Rational design of nickel hydroxide-based nanocrystals on graphene for ultrafast energy storage, Adv. Energy Mater. 8 (9) (2018) 1702247.
[293] H.R. Naderi, A. Sobhani-Nasab, M. Rahimi-Nasrabadi, M.R. Ganjali, Decoration of nitrogen-doped reduced graphene oxide with cobalt tungstate nanoparticles for use in high-performance supercapacitors, Appl. Surf. Sci. 423 (November) (2017) 1025–1034.
[294] B. Zhao, et al., A high-energy, long cycle-life hybrid supercapacitor based on graphene composite electrodes, Energy Storage Mater. 7 (2017) 32–39.
[295] S. Dai, et al., Controlled synthesis of three-phase NixSy/rGO nanoflake electrodes for hybrid supercapacitors with high energy and power density, Nano Energy 33 (2017) 522–531.
[296] B. Zhao, R. Ran, M. Liu, Z. Shao, A comprehensive review of Li4Ti5O12-based electrodes for lithium-ion batteries: the latest advancements and future perspectives, Mater. Sci. Eng. R Reports 98 (2015) 1–71.
[297] L. Guardia, et al., Biomass waste-carbon/reduced graphene oxide composite electrodes for enhanced supercapacitors, Electrochim. Acta 298 (2019) 910–917.